MODELLING AND DETECTION OF SHALLOW WATER - TARGETS

by

N. V. RAGHAVA RAO

DEPARTMENT OF ELECTRICAL ENGINEERING
INDIAN INSTITUTE OF TECHNOLOGY, KANPUR

JUNE, 1985

MODELLING AND DETECTION OF SHALLOW WATER - TARGETS

A Thesis Submitted
In Partial Fulfilment of the Requirements
for the Degree of
MASTER OF TECHNOLOGY

by

N. V. RAGHAVA RAO

to the

DEPARTMENT OF ELECTRICAL ENGINEERING
INDIAN INSTITUTE OF TECHNOLOGY, KANPUR
JUNE, 1985

ACKNOWLEDGEMENT

I am ~~grateful~~ grateful to my thesis supervisor, Dr. P.R.K. Rao for his guidance and encouragement given to me during the course of this work.

I am also, ~~grateful~~ grateful. to Director, NSTL, Vasakhapatnam for sponsoring me to this M.Tech. programme.

I am thankful to Mr. B. Venkataramani for the long discussions I had with him.

I finally acknowledge Mr. J.S. Rawat for his excellent typing of this thesis.

Kanpur
June, 1985

N.V. Raghava Rao

ABSTRACT

In this thesis an attempt is made to model the signal received from a target, such as a submarine, by an active SODAR, such as a homing torpedo. For an iso-speed shallow water channel, the channel exhibits discrete multipath scattering. For typical SODAR beam patterns and normally encountered boundary reflection losses, the number of paths with significant energies contributing to the received signal is small.

A characteristic feature of the above channel is seen to be the common doppler shift in the composite received signal due to target motion. This doppler shift is taken to be the average of all the doppler shifts of contributing rays as doppler ratio differences among paths are seen to be small.

Modelling the attenuation coefficients as Zeromean complex Gaussian random variables and modelling the random travel times with appropriate density functions, the optimum receiver is found to be too complex to be of practical interest. If perfect knowledge of arrival times is assumed, the optimum receiver is of simple nature. A conventional receiver under this characterization suffers no marked degradation. With an appropriate choice of envelope of the transmitting pulse, the optimum receiver implementation is simpler.

TABLE OF CONTENTS

CHAPTER 1

INTRODUCTION

The normally used receiver for the detection of a target in presence of white noise by an active SODAR (S und Detection And Ranging) is a correlation or a matched filter receiver. For such receivers the channel is considered to be dispersionless and unbounded, and the target is modelled as a slowly fluctuating point target. Then the return signal in an active SODAR is a replica of the transmitted pulse appropriately weighted and time delayed. Even if coloured noise is present, the same techniques used above suffice and it is generally observed that a suitable choice of transmitting waveforms will improve the receiver performance.

For bounded channels, there was no special mention on the performance changes for the above receivers. In this thesis we attempt to restructure the target and channel models when the channel is bounded and suggest some suitable receiver structures.

A bounded channel is assumed to have well defined closely spaced boundaries, (an example could be the shallow water channel where the source is operating at high frequencies) and such boundaries are said to produce specular reflection,

at high frequencies it is appropriate to characterize the reflection process to be regular and deterministic. Now in such a channel when the source/receiver and target are at fixed locations, the acoustic transmission may be described by ray theory and the channel is said to have a discrete multipath structure. Hence the received signal could be a super-position of weighted and time delayed replices of the transmitted pulse arriving at receiver after the 'reflection' at the target. In addition, a moving target will also introduce doppler shift on carrier frequency along each path. Hence the net effect of the channel and a target, which is modelled to have zeromean complex Gaussian reflection coefficient, is the spread of received energy over ambiguity plane. The amount of spreading of the received signal over ambiguity plane may be found by using ray tracing programmes even for a channel in which the sound transmission is a function of depth [1].

It is observed that the general interest in a multipath environment in a bounded channel is to investigate the coherence degradation between signals received at two remotely located sensors [2,3]. This scattering phenomena is some times applied in passive tracking of a moving

source in shallow waters [4,5]. An elegent model for the channel is suggested by Jacyna, Jacobson and Clark [5], where a passive source is tracked by two sensors.

In this thesis we adopt the Jacyna, Jacobson and Clark's model for an active SODAR to detect a moving target.

In certain occasions it is observed that special signal waveforms like coded pulse sequences or analog modulated waveforms (LFM etc.) are used in channels where thermal noise is a predominent component, for detection of targets. In this thesis we attempt to analyse the requirements of such waveforms when the channel is bounded.

In Chapter 1 of this thesis the problem under study is proposed. In Chapter 2 , we first review various concepts that are involved for computing the parameters needed in a multipath received signal formulation, and adopt a model for detecting a moving target in a shallow water channel for an active SODAR. In Chapter 3, we attempt to study the optimum receiver for the received signal characterized by random attenuation coefficients and random time of arrivals. We then observe the simplicity in optimum receiver design having a knowledge of time of arrivals. For this situation

we consider a conventional receiver and study the amount of its degradation compared to the optimum receiver. The effect of choice of transmitting waveforms are studied. In the end we discuss the results. In Chapter 4, we conclude the discussion with some suggestions for future work.

CHAPTER 2

MODELLING OF SHALLOW WATER TARGETS

2.1 INTRODUCTION:

In this chapter we are interested in developing a model for an under water SODAR target. Our concern is to characterize the signal received by an under water weapon system when it transmits a signal that is 'reflected' from a moving target. Such a situation for example, is encountered when an active torpedo homes onto a submarine moving in continental shelfs characterized by shallow waters.

The received signal features are dependent on the channel parameters which modify the acoustic propagation of the transmitted signal. Boundary conditions and channel parameters may have complex influence on the acoustic propagation. In Sec. 2.2, we consider the effect of various parameters of the medium on wave propagation and the relevance of ray acoustics to the present problem. In Sec. 2.3, we give expressions for travel time, spreading loss and reflection associated with an acoustic wave. In Sec. 2.4, we consider the multipath structure of the channel. The influence of a moving target and a general treatment to compute the return signal in a moving target environment is studied in Sec. 2.5. And finally in Sec. 2.6 we derive an

expression for the return signal for the above specified example and discuss the results obtained. Our account of the target model,in particular the influence of the source motion on the received acoustic field, closely follows the work of G.M. Jacyna, M.J. Jacobson and J.G. Clark [5].

2.2 UNDER-WATER ACOUSTIC PROPAGATION PRINCIPLES:

The acoustic wave propagation in an underwater channel is influenced by regular and random inhomogeneities of the medium [6]. Refraction, duct propagation etc. are the phenomena due to regular inhomogeneities. The regular inhomogeneities refer to the spatial and temporal variations in the mean characteristics like temperature, salinity and pressure etc. in the medium. In ocean media these effects are considerable in the direction of depth and the ocean medium is often said to have a layered structure. The random inhomogeneities on the other hand, cause phenomena like scattering or reverbaration. Which of the above two inhomogeneities is dominant depends on the specific situation under study. In this thesis we are mainly interested in regular inhomogeneities only.

The regular variations in temperature, salinity and pressure influence the magnitude of the velocity of propagation of the acoustic wave and consequently the path traversed by the acoustic wave.

We now briefly consider the basic principles which govern the acoustic propagation in the medium.

The propagation of sound in an under water channel can be described mathematically by the solution of the wave equation using the appropriate boundary and initial conditions for a particular problem. In a homogeneous and quiescent medium the velocity potential ϕ at a point on the wave obeys the wave equation given by [7]

$$\nabla^2 \phi - \frac{1}{c^2} \frac{\partial^2 \phi}{\partial t^2} = 0 \qquad (2.1)$$

where 'c' is the velocity of propagation of the wave and c is given as

$$c = (K/\rho_o)^{1/2}$$

where K is bulk modulus and ρ_o is density of the medium. The velocity of the particle on the wave is given by

$$v = \nabla \phi$$

and the pressure developed due to this velocity is given by

$$p = -\rho_o \frac{\partial \phi}{\partial t}$$

where ρ_o is the density of the medium.

Under the assumption of small perturbations in an ambient state, the above wave equation can easily be seen to follow from:

i) the principle of conservation of mass: This principle states that in a fluid the net rate of increase of mass per unit volume is equal to the rate of change of density. If $\rho(x,t)$ is the density of fluid at a point X and time t, v(x,t) is the fluid velocity at that point, the equation for conservation of mass is easily shown to be given by

$$\frac{\partial \rho}{\partial t} + \nabla \cdot (\rho v) = 0$$

ii) The Euler's equation of motion for a fluid: This equation states that the mass multiplied by accelaration of a fluid particle is equal to the net apparent forces exerted on it by it's environment and by external bodies. Neglecting the body forces such as gravity per unit mass, the equation of motion is written as

$$\rho \cdot \frac{\partial v}{\partial t} = -\nabla p$$

where p(x,t) is force per unit area or pressure.

iii) The equation of state: It describes the relation between the pressure of a fluid, and its density and temperature. If an excess pressure developed due to an acoustic wave is

Δp, then this excess pressure is proportional to the fractional change in density ($\Delta \rho$). Hence we write $\Delta p = K \cdot \Delta \rho$ where K is the bulk modulus of the medium.

There are two theoretical approaches to the solution of wave equation (2.1). One is called the normal mode theory [8], in which the wave propagation is described in terms of characteristic functions called normal modes, each of which is a solution of equation (2.1). In a bounded medium the standing wave pattern occurs due to super position of waves travelling in opposite directions towards boundaries. If H is the depth of the channel, then for all wavelength λ_j equal to $\frac{2}{j}H$ where $j = 1,2,3,\ldots$, a solution to wave equation is said to exist. In ocean media, the standing wave pattern occurs along the z-axis (depth) and the wave propagates along the x-axis (horizontal axis). The normal modes are combined additively to satisfy the boundary and initial conditions. With normal mode theory we obtain at a point and at a given time the combined effect of all wave paths. This analysis is relatively easy to handle when the number of modes is small. If the point at which the effect of the acoustic source is computed, is at a large distance (of the order of 50 Km) or the source frequency is small (less than 1000 Hz) the resulting number of modes will be small and normal mode theory may be applied.

The other approach to solving equation (2.1) is by ray theory [9]. Ray theory represents the acoustic field at a point as a sum of ray contributions, each ray emanating from the source and reaching the point after a certain number of boundary reflections. In media in which the sound velocity changes appreciably over a small distance (say in the order a wavelength of the sound wave), ray theory is not applicable. Hence ray theory may be seen to be applicable to high frequencies or short wavelengths in a practical situation. Ray tracing can be done using suitable computer programes for the energy loss, time of travel along each ray path [10].

An underwater weapon generally has the following operating specifications:

i) Source frequency range : 10 - 100 KHz

ii) Acquisition range : 2 - 3 KM

iii) Operating channel depths : 200 - 400 meters.

These factors allow us to use ray theory to analyse the received signal characteristics of an underwater weapon.

2.3 RAY ACOUSTICS:

We consider the wave equation in two dimensions, say x and z where x signifies the horizontal axis and z signifies

the depth, in a ocean medium. The positive direction of z is towards increasing depth. Let the acoustic source be producing a harmonic disturbance. We consider a homogeneous medium in which velocity of propagation of the acoustic wave 'c' is constant. Then the wave equation (2.1) is written as

$$\frac{\partial^2 \phi}{\partial x^2} + \frac{\partial^2 \phi}{\partial z^2} + \frac{\omega^2}{c^2} \phi = 0 \qquad (2.2)$$

consider

$$\phi(x,z,t) = \psi(z) \exp j(\pm\alpha x - \omega t) \qquad (2.3)$$

to be a solution of equation (2.2).

Equation (2.3) describes plane waves propagating in the direction of increasing x (+ sign) or decreasing x(- sign). The phase velocity of the wave is given by v and is equal to $\frac{\omega}{\alpha}$.

Substituting equation (2.3) in (2.2) gives the differential equation

$$\frac{d^2\psi}{dz^2} + \gamma^2\psi = 0 \qquad (2.4)$$

where

$$\gamma^2 = \frac{\omega^2}{c^2} - \alpha^2 = \alpha^2 \left(\frac{v^2}{c^2} - 1\right) \qquad (2.5)$$

Consider a solution of (2.4) as

$$\psi(z) = Ae^{j\gamma z} + Be^{-j\gamma z} \qquad (2.6)$$

where A and B are constants of integration.

Combining (2.6) and (2.3), we have

$$\phi(x,z,t) = A\, e^{j(\pm\alpha x+\gamma z-\omega t)} + B\, e^{j(\pm\alpha x-\gamma z-\omega t)} \qquad (2.7)$$

where the first term describes a wave travelling in the direction of increasing z, i.e., propagating down-wards and second term corresponds to a wave propagating upwards.

We write equation (2.5) as $\frac{\omega^2}{c^2} = \alpha^2 + \gamma^2$ and define

$$k^2 \triangleq \frac{\omega^2}{c^2} \qquad (2.8)$$

where k is the wave number in the direction of propagation. It is the magnitude of the vector K whose direction is normal to the wave front i.e., K defines the ray direction.

If we consider a plane wave described by an equation

$$\phi(x,z,t) = A\, e^{j(\alpha x+\gamma z-\omega t)}$$

then this plane wave is moving in a direction $\underline{K}$ whose magnitude k is given by $\sqrt{(\alpha^2+\gamma^2)}$ or inturn we can say that the plane wave is having α and γ as its x and z components.

Consider Fig. 2.1 and if θ is the angle the direction

of plane wave makes with z-axis, then the horizontal component $\alpha = k \sin\theta$ and vertical component $\gamma = k \cos\theta$. For a homogeneous medium we can see $\underline{K}$ is constant. That is the wave will not alter it's direction and it's magnitude remains constant as it propagates.

Now we derive a solution to the wave equation (2.2) in a medium where c is not a constant.

For a source producing harmonic disturbance consider a solution to the wave equation (2.2) as

$$\phi(x,z,t) = A(x,z)\ e^{j(S(x,z)-\omega t)} \qquad (2.9)$$

where S, a function of x and z to be determined. We substitute (2.9) into wave equation (2.2) and separate the real and the imaginary parts. Ignoring the time dependence, we have

$$\nabla^2 A - [(\frac{\partial S}{\partial x})^2 + (\frac{\partial S}{\partial y})^2]\ A + K^2 A = 0 \qquad (2.10)$$

and

$$2\ \nabla A \cdot \nabla S + A\nabla^2 S = 0 \qquad (2.11)$$

Rewriting (2.10) and (2.11) as

$$(\frac{\partial S}{\partial x})^2 + (\frac{\partial S}{\partial y})^2 - K^2 - \frac{\nabla^2 A}{A} = 0 \qquad (2.12)$$

and

$$\nabla^2 S + \frac{2}{A}\ \nabla A \cdot \nabla S = 0 \qquad (2.13)$$

If $\frac{\nabla^2 A}{A} \simeq 0$, then equation (2.12) implies

$$\left(\frac{\partial S}{\partial x}\right)^2 + \left(\frac{\partial S}{\partial y}\right)^2 = K^2 \qquad (2.14)$$

Equation (2.14) is called Eikonal equation (corresponding to the wave equation) and S(x,z) must satisfy (2.14). S(x,z), leading to a solution to the wave equation, if $\frac{2}{A} \nabla A . \nabla S$ is small in equation (2.13) must also satisfy

$$\nabla^2 S = 0 \qquad (2.15)$$

The general form of the solution of equations (2.14) and (2.15) will be

$$S(x,y) = c_1 x + \sqrt{(K^2 - c_1^2)}\, y \qquad (2.16)$$

where c_1 is a constant to be determined.

Equation (2.16) describes a plane wave front in which K is the wave number. It is the magnitude of a vector $\underline{K}$ whose direction describes the ray path. Let $\underline{K}$ make an angle θ with horizontal axis (x-axis), then we can show that $c_1 = K \cos\alpha$. This implies that c_1 is the direction cosine of $\underline{K}$ along x-axis.

Having obtained S(x,z), we substitute equation (2.9) now into wave equation and obtain a second order differential equation in A(x,z). Solving for A(x,z), we obtain $\phi(x,z)$

Conditions $\frac{\nabla^2 A}{A} \simeq 0$ and $\frac{2}{A}\nabla A \cdot \nabla S$ is small are satisfied, if the fractional changes in medium parameters like velocity are small over a wavelength. These conditions are generally met when the source operates at high frequencies.

The solution, (2.16) of eikonal equation is seen to be a plane wave with $K = \frac{\omega}{c}$. If velocity of sound 'c' is a function of x and z, the gradient of the wave front and therefore of the ray path change with x and z. Now we derive a condition which the ray path has to satisfy at each point.

Each point on the ray satisfies the eikonal equation $(\frac{\partial S}{\partial x})^2 + (\frac{\partial S}{\partial z})^2 = K^2 = \frac{\omega^2}{c^2}$.

An infinitesimal ray length can be described as

$$d\sigma = kdl = k(dx + dz)^{1/2} \qquad (2.17)$$

using Fermet's principle (which states that rays in physical space are paths of stationary time i.e., for small variations in path length between two fixed points, the resulting variations on the travel time integral $\int_{P_1}^{P_2} dt$ is zero); if the variation introduced on the path length between two fixed points we have $\delta \int d\sigma = 0$, then we have from equation (2.17), for $\omega \neq 0$

$$\delta \int K \, dl = \delta \int \frac{dl}{c} = 0 \qquad (2.18)$$

If we consider the velocity of wave 'c' to be a function of z only, which is true generally in ocean media, then writing $x_z = \frac{\partial x}{\partial z}$ equation (2.18) implies

$$\delta \int \frac{\sqrt{x_z^2 + 1}}{c(z)} \, dz = 0 \qquad (2.19)$$

Applying Euler-Lagranges formula, to equation (2.19) we have

$$\frac{d}{dz}\frac{\partial F}{\partial x_z} = 0 \qquad (2.20)$$

where $F \quad \frac{\sqrt{(x_z^2+1)}}{c(z)}$

Equation (2.20) implies $\frac{\partial F}{\partial x_z}$ = constant and we have

$$\frac{1}{c} \cdot \frac{x_z}{\sqrt{(x_z^2+1)}} = \text{constant } (=a) \qquad (2.21)$$

From Figure 2.2, if θ is the angle the ray makes with x-axis then

$$x_z = \frac{dx}{dz} = \cot\theta \qquad (2.22)$$

Therefore (2.21) implies, $\cos\theta/c(z) = a$

$$\frac{\cos\theta}{c(z)} = a \qquad (2.23)$$

Equation (2.23) is called Snell's law and it is to be satisfied at each point on the ray.

The eikonal equation in 3-D can be written as

$$(\frac{\partial S}{\partial x})^2 + (\frac{\partial S}{\partial y})^2 + (\frac{\partial S}{\partial z})^2 = K^2.$$

If we assume the velocity of the wave 'c' is a function of one co-ordinate only, namely z-coordinate, then for a ray

path, the direction cosines $\partial S/\partial x$ and $\partial S/\partial y$ along x and y co-ordinates must be constant at all points. This implies $\frac{(\partial S/\partial x)}{(\partial S/\partial y)}$ = constant and hence ray path is confined to a plane normal to xy plane. So with no loss of generality we assume the ray plane to be xz plane.

2.2.2 Computation of Travel Time and Spreading Loss:

We have seen in a medium in which 'c' is proportional to only z-co-ordinate, the rays are to be confined to xz plane only. We have also seen that at each point on the ray the Snell's law is satisfied. We now compute the horizontal distance (along x-axis) a ray traverses when it travels from a given depth (say $z_a = 0$) to another depth (say $z_a = z$), Equation (2.22) implies $dx = \cot\Theta\, dz$, and the horizontal distance traversed is given as

$$x = \int_0^z \cot\Theta\, dz \qquad (2.24)$$

$$= \int_0^z \frac{ac(z)}{\sqrt{(1-a^2c^2(z))}}\, dz \quad \text{(from equation (2.23))}$$

If 'c' is a linear function of z; i.e. writing c = pz, where p is the gradient, then equation (2.24) is evaluated and we have

$$X = \text{const.} \pm \frac{1}{ap}\,(1-a^2p^2z^2)^{1/2} \qquad (2.25)$$

Define $R \triangleq \frac{1}{ap}$ and $X_1 \triangleq$ const., the (2.25) implies

$$(X - X_1)^2 + Z^2 = R^2 \qquad (2.26)$$

Equation (2.26) implies that the acoustic ray traverses a circular path if 'c' is a linear function of depth. The radius of the circular path is $\frac{1}{ap}$ and the origin will lie at $(X_1,0)$ where z = 0 implies the depth where 'c' is extrapolated to zero. Fig. 2.3 illustrates the above statement.

Let θ be the angle of inclination the ray makes at the source with the horizontal axis. Let c_o be the velocity of propagation at the source. From equation (2.23) we have

$$\frac{\cos\theta}{c(z)} = a$$

Radius of curvature $R = \frac{1}{ap} = \frac{c}{p\cos\theta}$

and the origin lies at a depth where velocity profile extrapolates to zero or it is at a depth $\frac{c_o}{p}$ from the location of the source. Therefore centre of the circle is at $(X_1,0)$ where $X_1 = \frac{c_o}{p}\tan\theta$.

We define travel time along the path is equal to

$\frac{dS}{c}$ where $dS = \frac{dz}{\sin\theta}$ as may seen from Fig. 2.2.

Therefore if c is a linear function of z (i.e. , c = pz) then travel time 't' is given as

$$t = \frac{dz}{pz\sqrt{(1-a^2p^2z^2)}} \qquad (2.27)$$

Transmission loss along a ray path is a sum of spreading loss and attenuation loss. Attenuation loss includes losses due to absorption and scattering. In this discussion we ignore attenuation losses. Spreading loss is a geometrical effect representing the regular weakening of signal as it spreads outward from the source. In shallow water channels the medium is bounded by two surfaces and the spreading loss is assumed to be cylindrical loss and is given as [ ]

$$L^{-1} = \frac{1}{p} \cdot \frac{dA}{d\Omega}$$

where

p is the source energy per unit time per unit solid angle .

dA is the area swept out by the wave surface, normal to the ray at a horizontal distance x_o then

$$L^{-1} = \left| \frac{x}{p} \frac{\sin\theta}{\cos\theta_o} \frac{\partial x}{\partial \theta_o} \right|^{-1} \qquad (2.28)$$

where θ_o is the angle the ray path makes with the horizontal at the source and θ corresponds to the angle the ray makes with the horizontal at the point of interest.

2.3.2 Reflection Coefficient:

At the interface separating two media, the ray has to satisfy the following boundary conditions:

i) the vertical particle velocity must be continuous.

$$\frac{\partial \phi_1}{\partial z} = \frac{\partial \phi_2}{\partial z} \tag{2.29}$$

ii) continuity of pressure across the boundary is to be maintained, i.e.

$$\rho_1 \frac{\partial \phi_1}{\partial t} = \rho_2 \frac{\partial \phi_2}{\partial t} \tag{2.30}$$

where ρ_1 and ρ_2 are the densities of the media.

Define $\phi_{in} = A \exp(\alpha x + \gamma z - \omega t)$ as incident ray and $\phi_{re} = B \exp(\alpha x - \gamma z - \omega t)$ as the reflected ray. Refer Fig. 2.4.

Substituting above equations into boundary conditions, the reflection coefficient turns out to be

$$\frac{B}{A} = \frac{\frac{\rho_2}{\rho_1} - \left[\frac{(c_1/c_2)^2 - \cos^2\theta_1}{1 - \cos^2\theta_1}\right]^{1/2}}{\frac{\rho_2}{\rho_1} + \left[\frac{(c_1/c_2)^2 - \cos^2\theta_1}{1 - \cos^2\theta_1}\right]^{1/2}} \tag{2.31}$$

where c_1 and ρ_1 are the velocity of propagation and density of ocean medium and c_2 and ρ_2 corresponds to same quantities in the second medium.

Consider the second medium to be air and the interface to be ocean surface. Now the interface separates two media having large difference in their acoustic impedance. Acoustic impedance is defined as ρc, and we have $\rho_1 c_1 = 1.5 \times 10^5$ g/(cm)^2 sec. and $\rho_2 c_2 = 42$ gm/(cm)^{2}sec. (for air). So equation (2.31) implies that the reflection coefficient is unity and the reflected ray will have it's phase advanced by 180°.

On the other hand at the interface separating the sea and the sea bottom with ρ_2, c_2 as the parameters corresponding to the sea bottom, we have $c_1 < c_2$ and $\rho_1 < \rho_2$.

We define critical angle θ_c as

$$\cos \theta_c = \frac{c_1}{c_2} \qquad (2.32)$$

Now from equation (2.31) and (2.32) we see that the reflection coefficient will increase from a value equal to $\frac{\rho_2 c_2 - \rho_1 c_1}{\rho_2 c_2 + \rho_1 c_1}$ for $\theta = 90^\circ$ to a value, unity at angle of inclination $\theta = \theta_c$. A typical curve for reflectivity vs. inclination angle is shown in Fig. 2.5. For the angle of

inclination θ from θ_c to 0°, the reflection coefficient is purely imaginary with magnitude of the reflection coefficient being unity and the phase change is determined by inclination angle. The phase angle is given as

$$\epsilon = 2 \tan^{-1} \frac{\rho_1}{\rho_2} \left[\frac{\cos^2\theta - (c_1/c_2)^2}{1 - \cos^2\theta} \right]^{1/2} \qquad (2.33)$$

and ϵ is 0° at the critical angle and increases to 180° at $\theta = 0^\circ$.

2.3.3 Ray Displacement:

In general, the fields computed by the ray theory differ from those computed by the normal mode theory. Tindle and Bold [12] account for this discrepancy by the beam displacement suffered by rays on total reflection from the bottom. Total reflection means that for rays whose inclination angle are less than critical angle, the reflection coefficient amplitude is unity and has only phase change. And this additional phase is considered as extra path. When the extra path lengths and travel times are incorporated into the computation of acoustic fields, the two approaches were seen to give very nearly the same result.

Brokhovskikh [13] has shown that the lateral displacement Δ of a bounded beam for above situation is given

$$\Delta = - \partial\epsilon/\partial\alpha$$

where ϵ is the phase of the reflection coefficient given in (2.33) and is

$$\epsilon = 2 \tan^{-1} \left[\frac{\cos^2\theta - (c_1/c_2)^2}{1-\cos^2\theta} \right]^{1/2}$$

and α is the horizontal component of the wave number and is given as $\alpha = \frac{\omega}{c_1} \cos\theta$, where ω is the operating frequency of the source.

The time displacement τ associated with beam displacement is given as

$$\tau = \frac{\partial \epsilon}{\partial \omega}$$

Evaluating Δ and τ, we will have

$$\Delta = \frac{2 \rho_1 \rho_2 c_1 c_2 (c_2^2 - c_1^2) \cot\theta}{\omega (c_2^2 \cos^2\theta - c_1)^{1/2} (\rho_1^2 c_2^2 \cos^2\theta + \rho_2^2 c_1^2 \sin^2\theta - \rho_1^2 c_2^2)}$$

and

$$\tau = \frac{\rho_1 \rho_2 (c_2^2 - c_1)^2 \cot\theta \cos\theta}{\omega (c_2^2 \cos^2\theta - c_1)^{1/2} (\rho_1^2 c_2^2 \cos^2\theta + \rho_2^2 c_1^2 \sin^2\theta - \rho_1^2 c_1^2)}$$

For evaluating Δ and τ we make use of direction cosines given as

$$\gamma_1 = \frac{\omega}{c_1} \sin\theta$$

$$\gamma_2 = \frac{\omega}{c_1} \left(\cos^2\theta - \frac{c_1}{c_2} \right)^{1/2}$$

$$\alpha = \frac{\omega}{c_1} \cos\theta$$

θ being the angle the ray makes with horizontal.

Thus Δ is a function of frequency. The value of Δ is much less than a meter per reflection for frequencies that are of interest to this thesis. For moderately long ranges, the additional path to be considered is negligibly small and so the ray displacement contributions are ignored in further discussions. For example

for $f = 30$ KHz

we have $\Delta = 5$ cm.

2.4 MULTIPATH STRUCTURE OF THE CHANNEL:

Up to this point in this section, we developed various equations to compute ray path parameters. In this section we further investigate the nature of the ray paths.

In Section 2.3 we have seen that for a medium in which velocity profile is a complex function of depth, every point on the ray has to satisfy the Snell's law and a ray path is confined to a plane normal to xy plane. Thus the various ray paths can be traced in principle. Depending on the complexity of the profile and the permissible resolution between paths, for each ray starting from the source, we consider the range over which the velocity 'c' can be considered to be a constant or a linear function of depth. Accordingly we approximate the ray path either with a straight line or with an arc of circle. We trace the path considering

the successive segments over which velocity profile is approximated. Thus we can draw all the ray paths that eminate from the source. Depending on the location of target, we can compute the number of rays that intercept a target. For a given configuration of source and target locations and channel depth, we may be able to plot in finitely many paths connecting the source and the target.

For ease in handling, the following nomenclature is often adopted in classifying various rays. Among the group of rays that are obtained, we have a direct ray which is the line of sight ray. The remaining rays are ordered according to the number (n) of bottom reflections the ray has suffered. This number is called the order of the ray. Now n can have all integer values starting from zero. For n=0, i.e. for the zeroth order ray we have only one surface reflection. For each order of bottom reflection with $n \geq 1$, we can associate a set of four paths: one of them will be having n+1 surface reflections, another one will have n-1 surface reflection and two will have n surface reflections. The direct ray, and the rays having order n=0,1,2 are illustrated in Fig. 2.6.

We assume the velocity of sound c at a point in the medium is linearly proportional to the depth of the point in the medium. Depending on the positivity or negativity of the gradient, location of the source and the initial ray inclination,

each ray travels in one of the four characteristic ways. These categories are:

i) the ray which gets reflected at both the interfaces

ii) the ray which gets refracted at both the interfaces, i.e. the ray will not reach the interfaces but curves away due to the linear dependance of c on depth.

iii) the ray which gets reflected at surface and gets refracted at bottom (RSR)

iv) the ray which gets refracted at surface and gets reflected at bottom (RBR).

These four types of rays are illustrated in the Figure 2.7.

M.J. Jacobson [14] considered the ray paths under RSR and RBR categories and gave formulae to find the number of paths arriving at a given point from a source, path losses, path travel time and the initial inclination angles.

We now consider the approximations we make and the simplifications that result on ray path tracing in the channel of our interest.

We assume an iso-velocity shallow water channel which is having flat boundaries. Therefore ray paths travel in straight lines irrespective of the location of

the source and all rays belong to the category (i). The rays will have specular reflection at the boundaries. The direct ray will have spherical spreading and due to good reflectivity conditions assumed for boundaries, rest of the rays will have cylindrical spreading. Hence received energy decreases in proportion to the square of distance for targets at closer ranges and decreases in proportion to the distance for longer ranges. The under water weapons will be generally active in the ranges ranging from 500 meters to 2500 meters. Therefore on the average we assume the loss is due to cylindrical spreading.

From the discrete ray structure shown in Fig. 2.6, we can see that the direct ray arrives first at the target and is followed by either S ray or n=1 ray depending on the location of source and target. Then the higher order rays will arrive. As the order of the ray 'n' increases, the ray inclination at the source will become steeper. If the initial inclination is steeper than the critical angle (θ_c) defined in sec. 2.3.2, theray suffers reflection loss in magnitude. The number of rays that are to be considered are decided by the receiver and transmitter beam patterns. Among them we may neglect the rays that have inclination angles steeper than critical angle and undergo more bottom reflections.

On the average for a typical values of ρ_1, c_1, ρ_2, c_2 a ray suffers approximately 10 dB energy loss per bottom reflection of inclination angle exceeds critical angle.

Till now we consider the boundaries to be flat, but in a physical situation the bottom structure may have either positive slope or negative slope. The ray tracing can be carried out with a simple modification of the above procedure. This is discussed by G.V. Anand and P. Balasubramanian in their report [15].

2.5 EFFECT OF TARGET MOTION ON RECEIVED SIGNAL CHARACTERISTICS:

Using ray theory, we have seen that shallow water channel gives rise to a discrete multipath structure to the received signal. The received signal energy now is obtained by superposition of the energies arriving along these paths after getting 'reflected' at the target. If 'n' significant paths are to be considered each of the path energies may be characterized by an attenuation coefficient (A_n), arrival time (T_n) and initial path inclination angle (θ_n).

We now consider the effect of target motion. A moving target introduces a doppler shift in the frequency of the received signal with respect to the transmitted signal frequency. If $\underline{V}$ is the velocity associated with the target,

the doppler shift is defined in terms of the component of the velocity along the direct ray. We assume direct ray path length is large compared to the target movement over the time interval of interest and hence the only effect on the received signal is changing of phase with respect to receiver time frame 't' or equivalently doppler shift in the transmitted frequency.

We may now define a doppler shift (k_n) along each path by considering the velocity component of the target along that path and it may be given as

$$k_n = 2 \frac{\theta_n}{c} \omega_0$$

where θ_n is the velocity component of target motion along nth ray.

We now argue that difference between the doppler shifts of any two discrete paths is small as we view that the doppler shifts are due to the changes in the path lengths due to target motion. Hence we propose a common doppler shift for the total received signal which is independent of the order of the discrete ray path. We do this first by computing the phase of the received signal along each path and then showing that the change in phase of the combined signal is independent of the order of the constituent rays by using some valid approximations.

We first write an expression for the combined received signal in terms of it's constituent paths and for a general target motion.

Consider the geometry of the system as shown in the Fig. 2.8.

Let the transreceiver (TR) be located at origin 'O'. Suppose that the target at any instant of time follows a path σ with arbitrary velocity 'c', sound velocity could be a function of time. Target depth may change with time. Let the instantaneous position of the target (T_g) be given by P. Then OP is the slant range and is denoted as R(t). Consider the plane X'Z which contains the directed line OP. The projection of OP on OX' is OP' and is called horizontal range. The target is assumed to follow a path σ as shown and $\underline{V}(t) = \frac{dR(t)}{dt}$ is the velocity vector. We assumed that 'n' discrete ray paths eminate from transmitter, get 'reflected' at the target and arrive back at the receiver. We also assume that the return path from target traces the corresponding forward path. Let Θ_n be the angle nth ray (PR_n) which leaves the target, makes with OX'. The convention for the sign of angle we adopt is; Θ_n is positive if the ray travels in positive direction of z-axis (i.e., towards increasing depth) and Θ_n is negative if the ray travels towards decreasing z.

We have seen in Sec. 2.3.4 that the first ray to arrive at the receiver after reflection at target is direct ray. It is followed by rays having bottom reflections of order 'n' zero and onwards. Since the target is moving, the instantaneous position of P follows the path and accordingly the vertical planes containing different rays may be different.

Since the target is moving, the signal associated with nth ray at the receiver time 't' corresponds to a pulse reflected at a target position at an earlier time. For nth ray, let the ray leave the transmitter at time 't_n' and reach the receiver at time 't'. Then we have

$$t_n = t - 2\,T_n(t) \qquad (2.34)$$

where $T_n(t)$ is one-way travel time.

Here we see t_n to be direct function of t and so we may write

$$t_n = F_n(t) \qquad (2.35)$$

Let the transmitted signal is rectangular pulse with carrier frequency ω_o.

write,

$$s(t) = \mathrm{Re}[\mathrm{Exp}\ (j\omega_o t)] \quad 0 \leq t \leq T \qquad (2.36)$$

Now the received signal along nth ray is written as

$$r_n(t)=\mathrm{Re}[A_n(t-T_n(t))\exp\ j(\omega_o(t-2\ T_n(t)+S_n(t))\ ] \tag{2.37}$$

where $A_n(.)$ is the attenuation coefficient along the path. This includes path losses and reflection coefficient of the target γ_n. $S_n(t)$ is the phase introduced due to boundary reflections and also includes the phase (δ_n) of complex reflection coefficientof the target. The nth ray may have N bottom reflections and M surface reflections along it's path. Then

$$S_n(t) = N_n(t)\epsilon_n(t) + \pi M_n(t) + \delta_n \tag{2.38}$$

where ϵ_n is the phase change per one bottom reflection. Each surface reflection introduces a phase change of π. In principle number of reflections and phase change due to bottom reflection could be functions of time.

$A_n(.)$ is given as

$$A_n(t) = |\tilde{a}_n|\ \ L_n^{-1}(t)\ [B_n(t)]^{N_n(t)} \tag{2.39}$$

where $L_n^{-1}(t)$ is two way spreading loss and we assume the path length difference in forward and backward paths is negligible over the analysis interval.

$B_n(t)$ is the path loss due to one bottom reflection $|a_n|$ is the modulus value of complex reflection co-efficient.

Now we want to represent the received signal as a complex envelope with an associated carrier frequency ω_o. First we write

$$r(t) = Re[\Sigma A_n(t) \exp j\{\omega_o t - 2\omega_o T_n(t) + S_n(t)\}]$$

$$= Re[\Sigma A_n(t) \exp j(\omega_o t - \phi_n(t)] \qquad (2.40)$$

where $$\phi_n(t) = -2\omega_o T_n(t) + S_n(t) \qquad (2.41)$$

Then we write

$$r(t) = A(t) \exp j(\omega_o t + \phi(t) \qquad (2.42)$$

Therefore,

$$A(t) = [\Sigma A_n^{(t)} \sin\phi_n(t)]^2 + [\Sigma A_n(t) \cos \phi_n(t)]^2 \qquad (2.43)$$

and

$$\phi(t) = \tan^{-1} \frac{\Sigma A_n(t) \sin \phi_n(t)}{\Sigma A_n(t) \cos \phi_n(t)} \qquad (2.44)$$

We now introduce some assumptions and approximations and derive the composite signal for the case of interest to us.

2.5 ISO-SPEED CHANNEL:

We assume that the velocity of propagation 'c' is a constant throughout the medium. The channel is bounded by

horizontal boundaries. The target is assumed to follow a horizontal straight line path with constant speed v.

As shown in Fig. 2.9, let P be the location of the transreceiver and Q be the location of target at t=0. Now R_o PQ gives the slant range at t=0. Let PQ' R_{HO} be the horizontal range at t=0, and γ be the angle which the target path projected on to the horizontal plane makes with PQ' at t=0. R is the instantaneous position of target and R(t) is the instantaneous slant range. It's projection on XY plane is $R_H(t)$.

From Fig. 2.10 we observe, transreceiver 'P' is at a depth of H_R, target is at a depth of H_T and the channel depth is H. Vertical height of PQ is 'n'. As we have seen previously, each order of reflection is associated with a set of four rays. Each ray is characterized by its initial inclination. If θ_n is the angle mode by the nth ray, we follow a convention and say $\theta_n > 0$ and $\alpha = +1$, if the ray leaves the source downward; else $\theta_n < 0$ and $\alpha = -1$, and also $\beta = +1$ if the ray reaches target/receiver from above, else $\beta = -1$. This convention helps in calculating path lengths easily. Some typical ray paths in a moving target environment are shown in Fig. 2.10. Here the rays may not lie in the same plane.

First we calculate the ray path length (one way) for N bottom reflections assuming target is stationary. For this we can use the method of images of the source that contribute energy at the target. Each ray may be identified by considering the number of times it crosses the surface and bottom or their images. From the Fig. 2.11 we see that

$$R_{no} = \text{nth ray path length}$$
$$= [R_o^2+(2NH+\alpha H_R + \beta H_T)^2]^{1/2} \qquad (2.45)$$

where N is the number of bottom reflections and R_o is the direct ray length.

In Fig. 2.11, the line segment from pto O indicates the Oth order ray path (surface reflection only) and line segments from pto 1_A, 1_B, 1_C, 1_D denote the set of 1st order ray paths. Ray path lengths can be easily computed from the geometry. For example, Ray $_A$ corresponds a path having two surface reflections and one bottom reflection. Its length is given as $[R_o^2+(2H + H_T + H_S)^2]^{1/2}$.

Therefore equation (2.45) gives nth ray path length as R_{no} for a target at rest. Then one way travel time is given as

$$T_{no} = \frac{R_{no}}{c} \qquad (2.46)$$

From Fig. 2.9 we can compute the path length for nth ray for a moving target.

$$R_n(t) = [R_{no}^2 + v^2 t_n^2 + 2vt_n R_{HO} \cos\gamma]^{1/2}$$

$$= [c^2 T_{no}^2 + v^2 t_n^2 + 2vt_n R_o(1 - \frac{h^2}{R_o^2})^{1/2} \cos\gamma]^{1/2}$$

where $h = H_T - H_S$ (2.47)

From equation (2.34) we write now

$$t_n = t - 2T_n(t_n)$$

$$= t - 2c^{-1}[(v t_n)^2 + 2 R_o v t_n(1 - \frac{h^2}{R_o^2})^{1/2} \cos\gamma + c^2 T_{no}^2]^{1/2}$$

$$= t - 2[M^2 t_n^2 + 2R_o c^{-1} M t_n(1 - \frac{h^2}{R_o^2})^{1/2} \cos\gamma + T_{no}^2]^{1/2} \quad (2.48)$$

where M is called mach number and defined as

$$M = \frac{v}{c} \quad (2.49)$$

Solving equation (2.48) as a quadratic equation we have

$$t_n(t) = F_n(t) = [t + 4 R_o M(1 - \frac{h^2}{R_o^2})^{1/2} c^{-1} \cos\gamma]$$

$$- [4 T_{no}^2 + 8 R_o M t (1- \frac{h^2}{R_o^2})^{1/2} c^{-1} \cos\gamma +$$

$$4M^2(t^2-4T_{no}^2 + 4(R_o^2-h^2) c^{-2} \cos^2\gamma)]^{1/2} x$$

$$x (1-4M^2)^{-1} \qquad (2.50)$$

If we make realistic assumption now like $M << 1$ and $H << R_o$ (i.e., velocity of target is much smaller than velocity of sound and depth of the channel is much smaller than range), then equation (2.50) simplifies to

$$F_n(t) = t + 4R_o M c^{-1} \cos\gamma - 2(T_{no}^2 + 2R_o M c^{-1}(\cos\gamma)t$$

$$+ M^2 t^2)^{1/2} \qquad (2.51)$$

$F_n(t)$ is the transmitted pulse time frame ('t_n') which has limits $0 \leq F_n(t) \leq T$ where T is the pulsewidth. We expand $t_n(F_n(t))$ using Maclaurin's series.

$$F_n(t) = t-2T_{no} + 4 R_o M c^{-1} \cos\gamma - \frac{2R_o M c^{-1}\cos\gamma}{T_{no}} t \qquad (2.52)$$

Consider $t(1 - \frac{2R_o M c^{-1}\cos\gamma}{T_{no}})$ in equation (2.52), where T_{no} is the travel time of nth ray when target is stationary and it will be in the order of $2R_o c^{-1}$. Even for $\cos\gamma = 1$, $\frac{2R_o M c^{-1} \cos\gamma}{T_{no}}$ is negligable compared to '1' if $M << 1$.

Therefore, we write

$$F_n(t) = t - 2T_{no} + 4R_o M\, c^{-1} \cos\gamma \qquad (2.53)$$

where $t = 0\ (2R_o/c)$.

We now proceed to find expressions for the attenuation coefficients, phases and inclination angles associated with various rays.

The inclination angle Θ_n for the nth ray is easily seen from the geometry of Fig. 2.11 as

$$\Theta_n = \tan^{-1}\left[\frac{\beta H_T - \alpha H_R + 2N_n H}{\alpha R_n + R}\right] \qquad (2.54)$$

Spreading loss associated with nth ray is computed with the assumption that they on the average are cylindrical losses, we have for one way path from equation (2.28).

$$L_n^{-1/2}(t) = |\text{nth ray path length}|^{-1/2}$$

$$= c^{-1}\left|T_{no}^2 + M^2 t_n^2 + 2R_o c^{-1} M(\cos\gamma)\, t_n\right|^{-1/2} \qquad (2.55)$$

Let B_n be the boundary reflection loss of nth ray per one bottom reflection derived from equation (2.31). Then for N_n bottom reflections along nth ray we have total boundary loss $= [B_n]^{N_n}$.

Therefore total amplitude loss is given as

$$\bar{A}_n(t) = [B_n]^{N_n} L_n^{-1}(t) \mid \tilde{a}_n \mid \qquad (2.56)$$

where a_n is the complex reflection coefficient of the target.

Now we linearize $L_n^{-1}(t)$ as follows:

$$L_n^{-1}(t) = c^{-2}[T_{no}^2 + M^2 F_n^2(t) + 2R_o M F_n(t) c^{-1} \cos\gamma]^{-1}$$

$$= c^{-2} T_{no}^{-2} \left[1 + \frac{M^2 F_n^2(t) + 2R_o M F_n(t) c^{-1}\cos\gamma}{T_{no}^2}\right]^{-1} \qquad (2.57)$$

Again using the procedure in simplifying (2.51) we have

$$L_n^{-1}(t) = c^{-2} T_{no}^2 \left(1 - 2M \cos\gamma \left(\frac{ct}{R_o} - 2\right)\right) \qquad (2.58)$$

where T_{no} is the order of R_o/c.

Hence total loss $A_n(t)$ is given as

$$A_n(t) = [B_n]^{N_n} |\tilde{a}_n| (c\, T_{no})^{-2} \left(1 - 2M \cos\gamma\left(\frac{ct}{R_o} - 2\right)\right) \qquad (2.59)$$

The total phase is given as

$$S_n(t) = \left[N + \frac{|\beta - \alpha|}{2}\right] \pi + N\epsilon + \delta_n \qquad (2.60)$$

where first term gives the phase change due to surface reflections and second term gives the phase change due to

bottom reflections and ϵ is the phase advance due to one botton reflection. Here we assume the number of reflections N_n and phase change ϵ are not function of time as the order n of the ray is not large. Hence $S_n(t)$ is not a function of time.

Knowing the values of $A_n(t)$, S_n and $T_n(t)$, the received signal contribution from the nth ray can be computed. It is given as

$$r_n(t) = Re[A_n(t) \exp j\{\omega_o(t-2T_n(t)) + S_n\}],$$

$$= Re[A_n(t) \exp j\{\omega_o t + \phi_n(t)\}] \qquad (2.61)$$

where,

$$\phi_n(t) = -2\omega_o[T_{no}^2+M^2F_n^2(t)+2R_oM\,F_n(t)c^{-1}\cos\gamma]^{1/2} \qquad (2.62)$$

Consider the expression given in square brackets in the above equation; and using the simplification procedure adopted in case of equation (2.51), we will have

$$\phi_n(t) = -2\omega_o[T_{no} + M(\cos\gamma)t-2R_o\,M\,c^{-1}\cos\gamma]+S_n \qquad (2.63)$$

Now we write the total acoustic field received as

$$r(t) = \mathrm{Re}\Big[\sum_n [B_n]^{N_n} |\tilde{a}_n| \, (CT_{no})^{-2}(1-2M\cos\gamma(\frac{ct}{R_o} -2)$$

$$x \exp j\{ \omega_o t - 2\,\omega_o T_{no} - 2\omega_o M(\cos\gamma)t + 4\omega_o R_o M c^{-1} \cos\gamma + S_n\}\Big]$$

Rewriting the above equation as

$$r(t) = \mathrm{Re}\Big\{\Big[[i -2M\cos\gamma(\frac{ct}{R_o} -2))\exp j(-2\omega_o M(\cos\gamma)t$$

$$+ 4\omega_o R_o M c^{-1}\cos\gamma)\Big] x\Big[\sum_n [B_n]^{N_n}|a_n|(c\,T_{no})^{-2}$$

$$\exp j(-2\,\omega_o T_{no}+S_n)\Big] x\, e^{j\omega_o t}\Big]\Big\} \qquad (2.64)$$

Thus the received signal is seen to be the product of two terms, one of which is a function of the target velocity alone and the other - under the summation sign - is the composite signal corresponding to a target at rest. Denoting the later term by $A_o \exp(j\phi_o)$ we write

$$A_o \exp(j\phi_o) = \sum_n [B_n]^{N_n}|a_n| \, (cT_{no})^{-2}\exp j(-2\omega_o T_{no}+S_n)$$

(2.65)

Now we have

$$r(t) = \mathrm{Re}\{[(1-2M\cos\gamma\,(\frac{ct}{R_o} -2))\, A_o \exp j(-2\omega_o\, M(\cos\gamma)t$$

$$+ 4\,\omega_o R_o\, M\, c^{-1}\cos\gamma + \phi_o)]\, e^{j\omega_o t}\} \qquad (2.66)$$

Comparing with the above, the $\mathbf{r}(t)$ given in equation (2.42) we observe

$$\phi(t) = \phi_o - 2\,\omega_o\, M \cos\gamma\,(t-2R_o c^{-1}) \tag{2.67}$$

and

$$A(t) = A_o\;\; 1-2M\cos\gamma\,(\frac{ct}{R_o} - 2) \tag{2.68}$$

We thus finally have, as $M \ll 1$,

$$\mathbf{r}(t) = \mathrm{Re}\;\; [A_o \exp j(\phi_c - 2\omega_o\, M \cos\gamma(t-2R_o c^{-1}))]e^{j\omega_o t} \tag{2.69}$$

or write

$$\mathbf{r}(t) = \mathrm{Re}\;\; [A_o \exp j(+\,\omega_D t)\exp j(\phi_o - 4\omega_o\, M \cos\gamma\, R_o c^{-1})]\; e^{j\omega_o t} \tag{2.70}$$

where,

$$\omega_D = -2\,\omega_o\, M(\cos\gamma)t \tag{2.71}$$

We now observe that the doppler frequency (ω_D), we obtained in the analysis is same as the doppler frequency one obtains in classical sense for a situation where the target is moving radially.

Rewriting equation (2.70) as

$$\mathbf{r}(t) = \mathrm{Re}\;\; [A_o \exp j(\phi_o - 4\omega_o M \cos\gamma\, R_o c^{-1})]\, \exp j(\omega_o + \omega_D)t \tag{2.72}$$

In the above equation, the term,

$$\phi_o - 4\omega_o M \cos\gamma\, R_o c^{-1} = -2\omega_o T_{no} - 4\omega_o M \cos\gamma\, R_o c^{-1} + S_n .$$

Since $M \ll 1$ and T_{no} is in the order of $R_o c^{-1}$, we simplify it as $\phi_o(0)$.

Therefore,

$$r(t) = \mathrm{Re}\ \left[\Sigma\, [B_n]^{N_n} |a_n]\ (c\, T_{no})^{-2} \exp(-2\omega_o T_{no} + S_n)\right]$$

$$\exp j(\omega_o + \omega_D)t \qquad (2.73)$$

Therefore the composite received signal for a moving target situation is seen to have amplitude equal to the amplitude computed when the target is assumed to be at rest, and having a carrier frequency shifted by ω_D from transmitted frequency ω_o, where ω_D is due to a moving target.

2.7. Results:

We want to investigate the variations on time delay differences τ_i and attenuation coefficients $|a_i|$ in a shallow water channel with known source and target depths.

The values of the parameters we consider below are typical to a situation where a torpedo is homing on to a submarine. The following parameters are assumed:

i) Velocity of propagation in the channel : $c_1 = 1500$ m/sec.

ii) Velocity of propagation in channel sediment: $c_2 = 1600$m/sec.

iii) Density of the channel : $\rho_1 = 1000$ gm/cm^3.

iv) Density of the channel sediment : $\rho_2 = 1250$ gm/cm^3.

v) Channel depth : H = 300 m.

vi) Source frequency : f = 30 KHz.

vii) Transmitting pulse width : T = 100 msec.

viii) Target velocity : V = 15 m/sec.

ix) Direction of moving target : $\gamma = 75^\circ$.

x) Target range : R = 500 - 1000 - 1500 - 2000m.

xi) Target depth : H_T = 0 - 50 - 100 - 150 - 200 - 250-300m.

xii) Source depth : H_R = 50 - 150 - 250.

xiii) Beam pattern : Vertical : 40°; Horizontal : 80°.

xiv) Target strength : IF $70^{\circ} < \gamma < 90^{\circ}$: TS = 300

else IF $0^{\circ} < \theta_n < 10^{\circ}$: TS = 30

$10^{\circ} < \theta_n < 20^{\circ}$: TS = 35

$20^{\circ} < \theta_n < 45^{\circ}$: TS = 60

$45^{\circ} < \theta_n < 90^{\circ}$: TS = 150

We compute the desired parameter values, for direct ray and the sets of reflected rays with order N = 0,1,2,3. It is observed that for $N \geq 3$, the inclination angle θ_n of the rays are out of beam pattern.

The following parameters are computed for each ray and the equations which are used are shown in brackets.

i) Critical angle (θ_c) : from equation (2.32)

ii) Inclination angle (θ_n) : from equation (2.54)

iii) Time of travel (T) : from equation (2.46)

iv) Spreading loss (SPLS) : from equation (2.55)

v) Boundary reflection loss(BLS): from equation (2.31)

vi) Bottom reflection phase ϵ : from equation (2.33)

vii) Total phase introduced due to boundary reflection : $N\epsilon + M\pi$

where M is the number of surface reflections.

viii) Array factor AF : using θ_n and Beam pattern specifications

ix) Target strength: TS: Using γ, θ_n and target strength specifications.

x) Total attenuation coefficient $|\hat{a}'_i|$: SPLS x BLS x AF x TS.

Then normalizing the parameters T and $|\tilde{a}_i|$ with respect to direct ray parameters, we compute time delay differences and normalized attenuation coefficients $|\tilde{b}_i|$ as

$$\tau_i = T_i - T_d$$

$$\text{and} \quad |\tilde{b}_i| = \frac{|\tilde{a}_i|}{|\tilde{a}_d|}$$

where T_d and $|\tilde{a}_d|$ refer to the direct ray.

The following results are observed:

1. For a given range of the target and source depth, time delay difference (τ_i) of any ray path is linearly dependent on target depth (since the linearized version of the equation (2.45) is used). The gradient of the ray depends on the type of the ray. Refer graphs 2.1 and 2.2.

2. For a given source and target depths, the time delay differences (τ_i) depend non-linearly on range of the target. Refer graph 2.3.

3. For a given source and target depths; graph 2.4 shows the attenuation loss with respect to range.

4. The spreads of time delay differences for various rays are shown in Table 2.1 The rays that have higher

order have larger spread; i.e., if τ_i are arranged in increasing order, then we observe

$$\Delta\tau_i < \Delta\tau_j \quad \text{for } \tau_i < \tau_j$$

where Δ_i is the spread of the delay τ_i.
This fact will be useful in Chapter 3, in computing the correlation coefficients and their probability densities, among signals which arrive along different paths.

5. The number of significant paths that contribute to the composite received signal at each range are shown in Table 2.2.

6. Assuming each range bin is of transmission pulsewidth 'T', starting from direct ray time delay $2T_d$, the time delay differences are arranged in corresponding range bins. This observation is helpful to see how the return signal energies via different paths are distributed. Some typical results are tabulated in Table 2.2.

7. Table 2.3 gives the type of rays that contribute to received signal at each given range. We observe that the number of rays contributing to the channel are same irrespective of source and target depths. The only change we see for 1000 m and 1500 m., is due to the

the symmetry of ray paths with respective to source and target depths. This result will be useful in estimating the arrival times as will be discussed in Chapter 3.

8. In Graph $\angle^{(2.1,2.2)}$ we observe at a given range and source depth, the variations in time delay differences. The values taken for range (R); source depth (H_R) and target depth (H_T) are arbitrary but typical. We observed that some time delay differences (τ_2, τ_5, τ_6 etc.) are increasing with respect to target depth whereas the other time delay differences (τ_3, τ_4, etc.) are decreasing with increase in target depth. This implies that as H_T changes some paths are moving away from direct ray and some are moving closer. Therefore $\angle^{\text{for}}$ a change in H_T, there is a net amount of change in this movement. This result will be of considerable importance to analyze the performance of conventional result in Chapter 3.

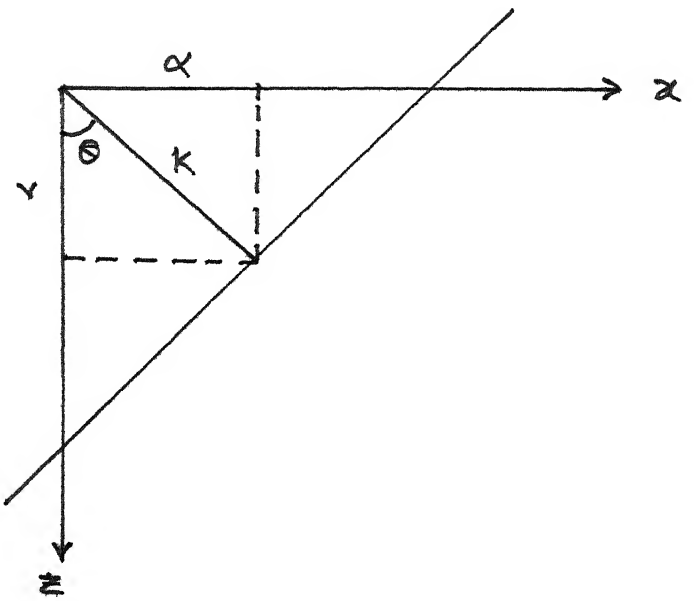

FIG 2·1 DIRECTION COSINES OF A PLANE WAVE.

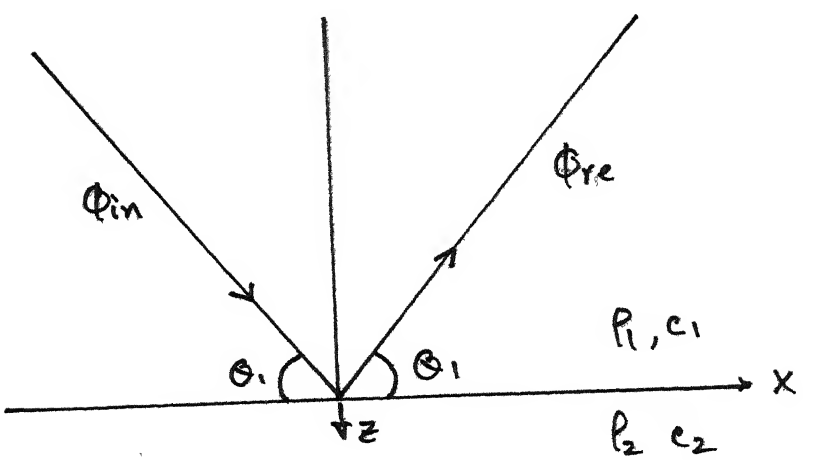

FIG 2·4 BOUNDARY REFLECTIONS AT BOTTOM

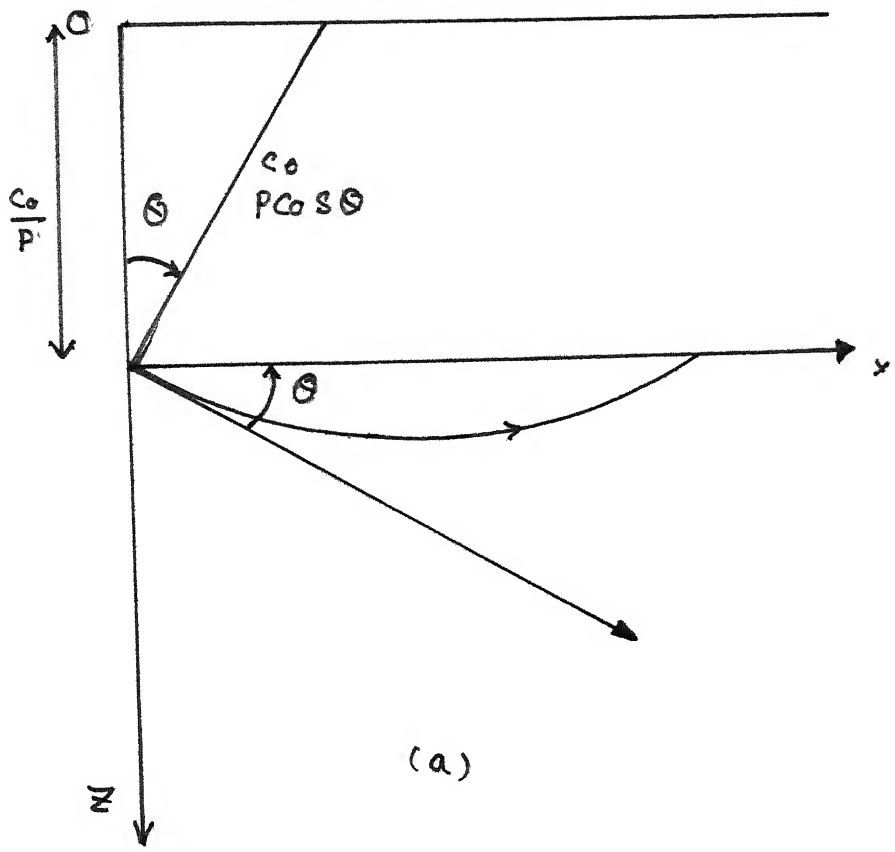

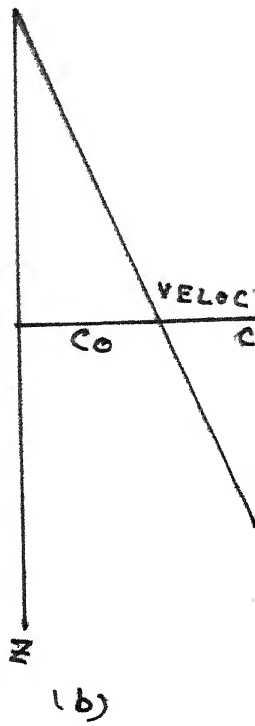

2.3 : (a) GEOMETRICAL RAY TRACING OF A RAY WITH ANGLE Θ

(b) VELOCITY PROFILE OF THE MEDIUM.

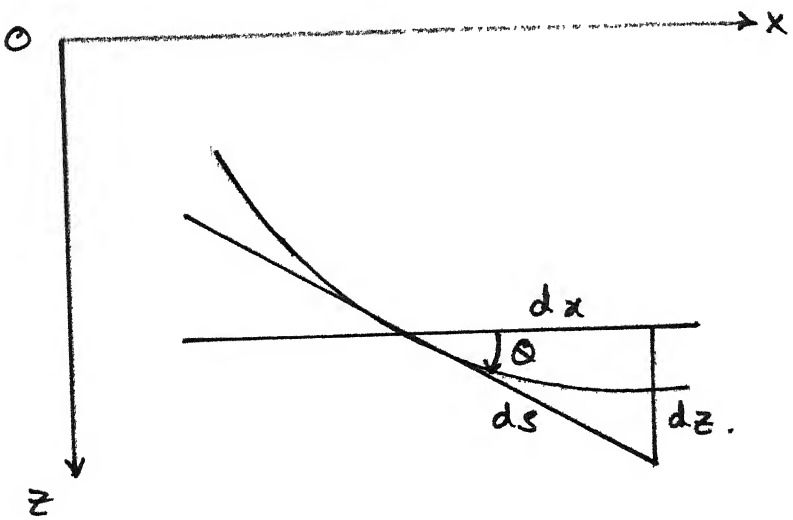

§ 2.2 : DIRECTION COSINES OF RAYPATH

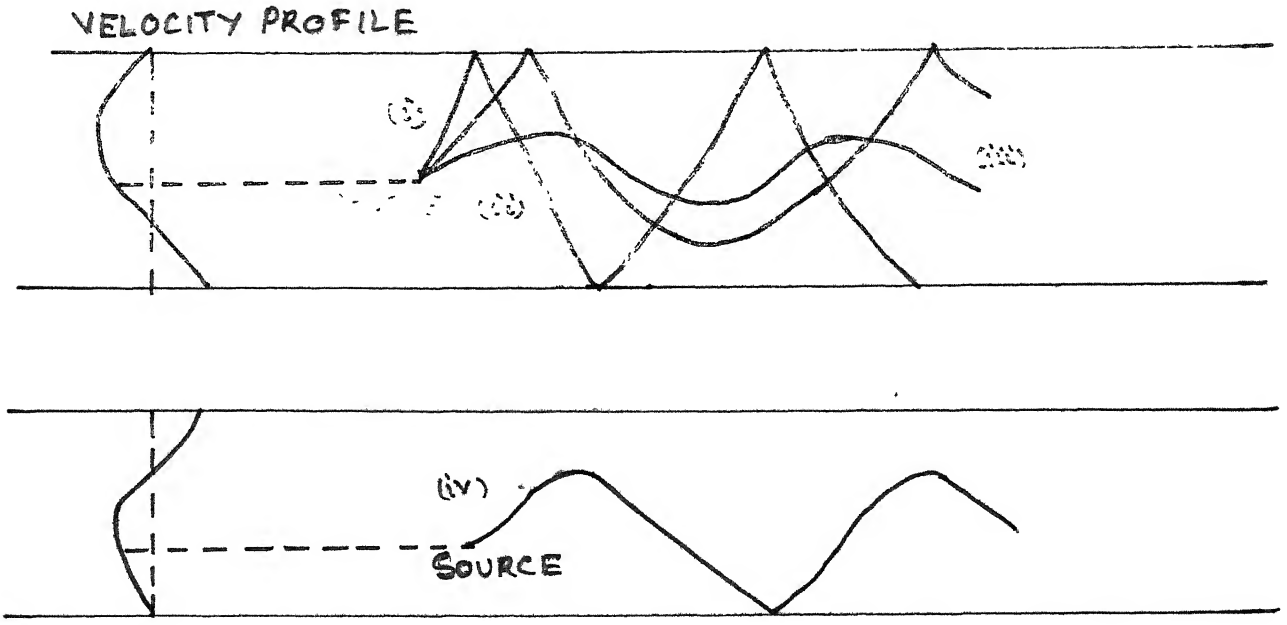

FIG. 2.7 RAY PATHS IN A CHANNEL HAVING NON-LINEAR SOUND VELOCITY PROFILE.

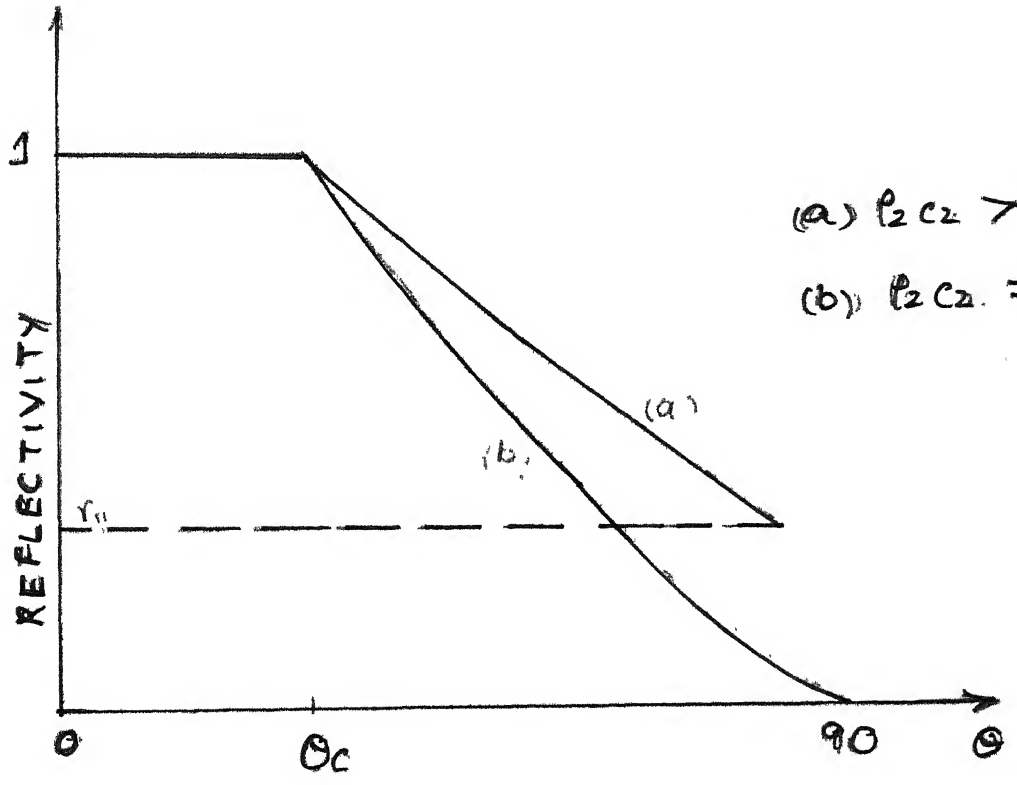

(a) $\rho_2 c_2 > \rho_1 c_1$ | $c_2 > c$

(b) $\rho_2 c_2 = \rho_1 c_1$

FIG 2.5 REFLECTIVITY VS INCIDENT ANGLE.

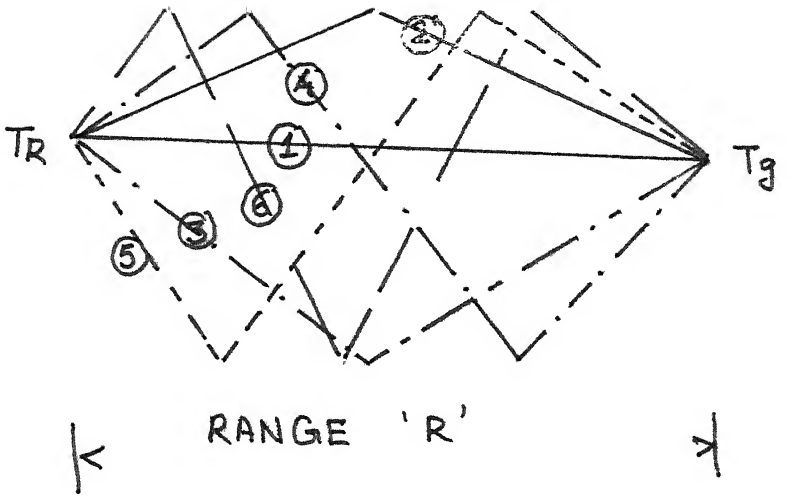

IG 2·6(a) RAY DIAGRAMS FOR DIRECT RAY AND RAYS OF ORDER 0 AND 1

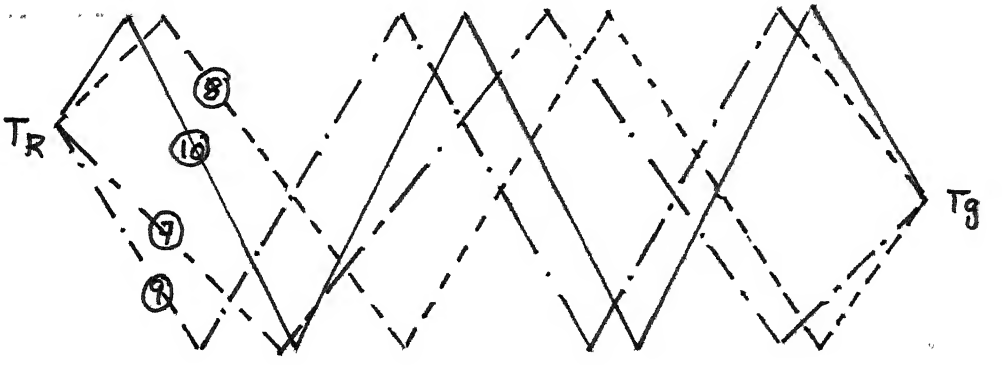

:IG 2·6(b) RAY DIAGRAM FOR THE 2ND ORDER RAY.

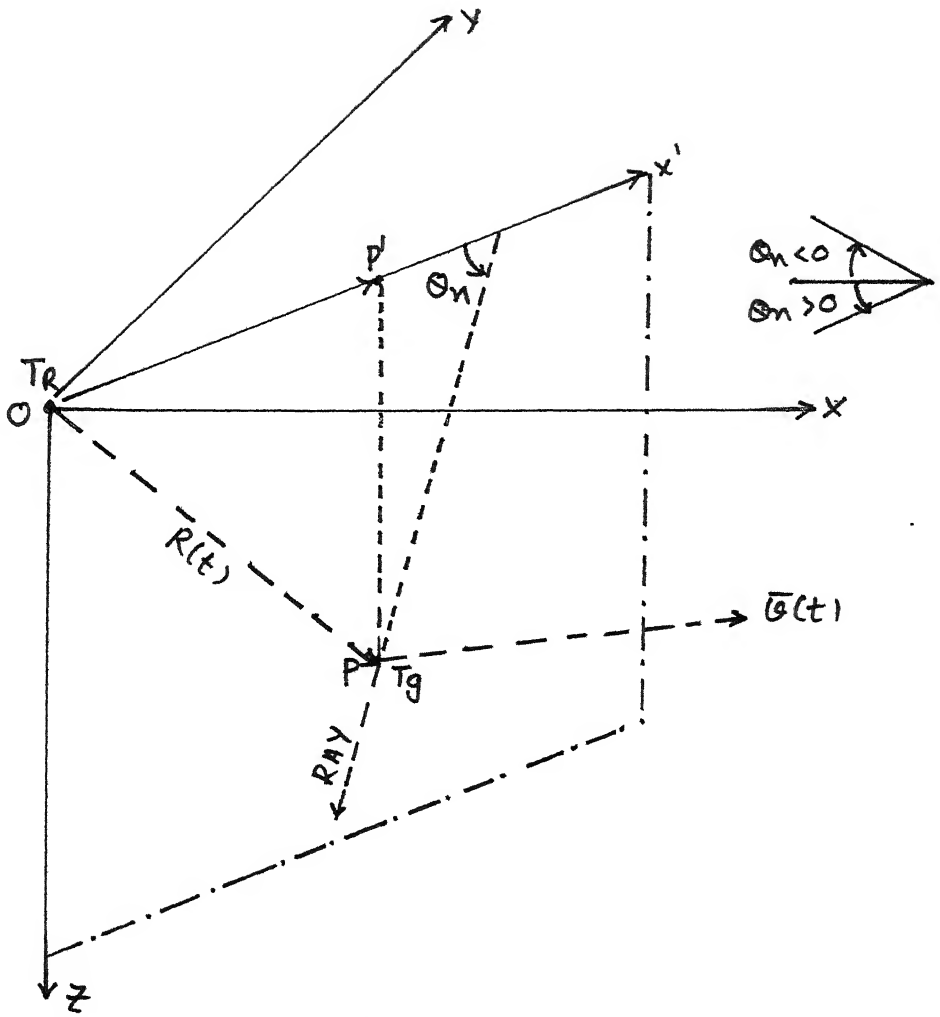

Fig 2.8 GENERAL GEOMETRY FOR A MOVING TARGET AND FIXED RECEIVER.

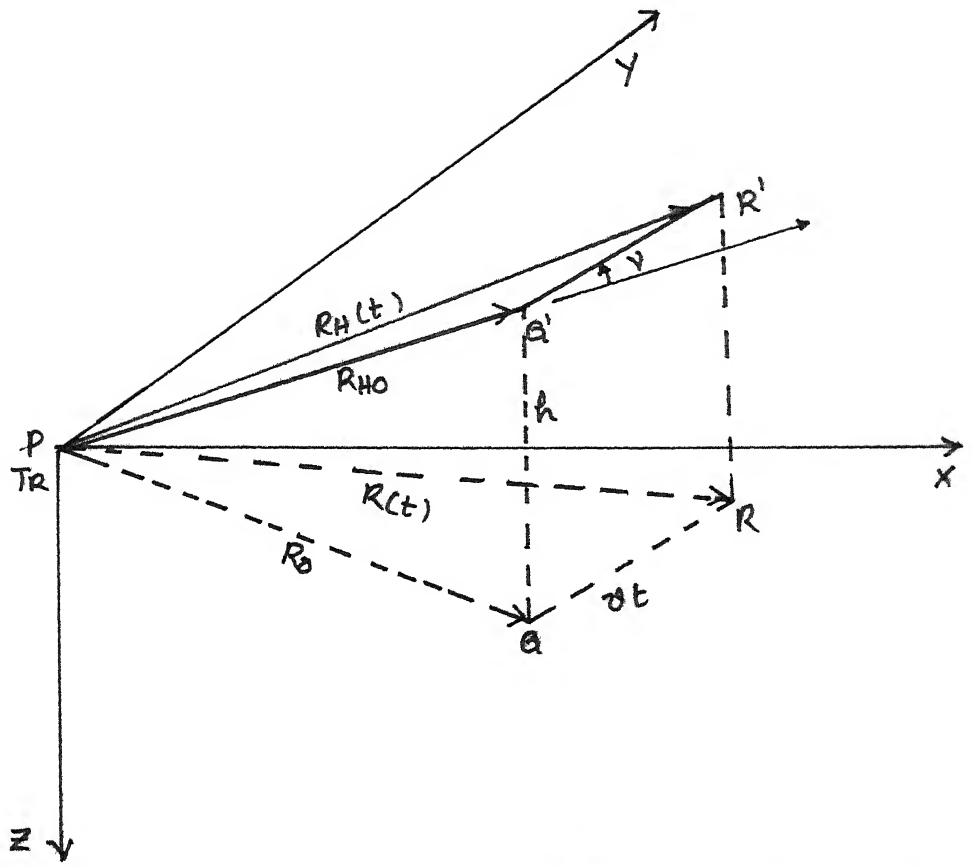

IG 2.8 GEOMETRY FOR LINEAR, CONSTANT SPEED TARGET MOTION IN AN ISOSPEED CHANNEL.

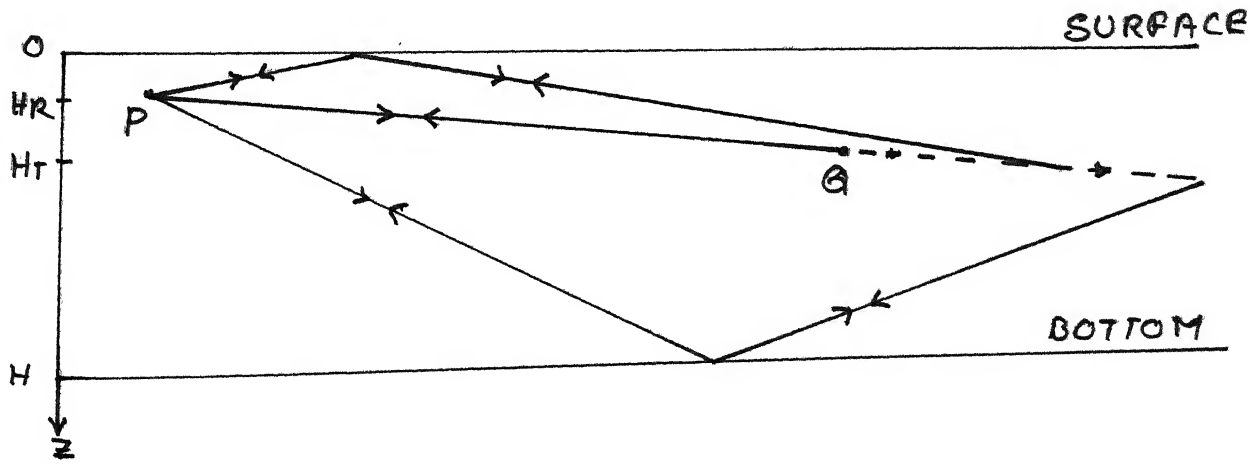

FIG 2.10 FRONT VIEW OF THE FIRST THREE RAYS IN THE CHANNEL.

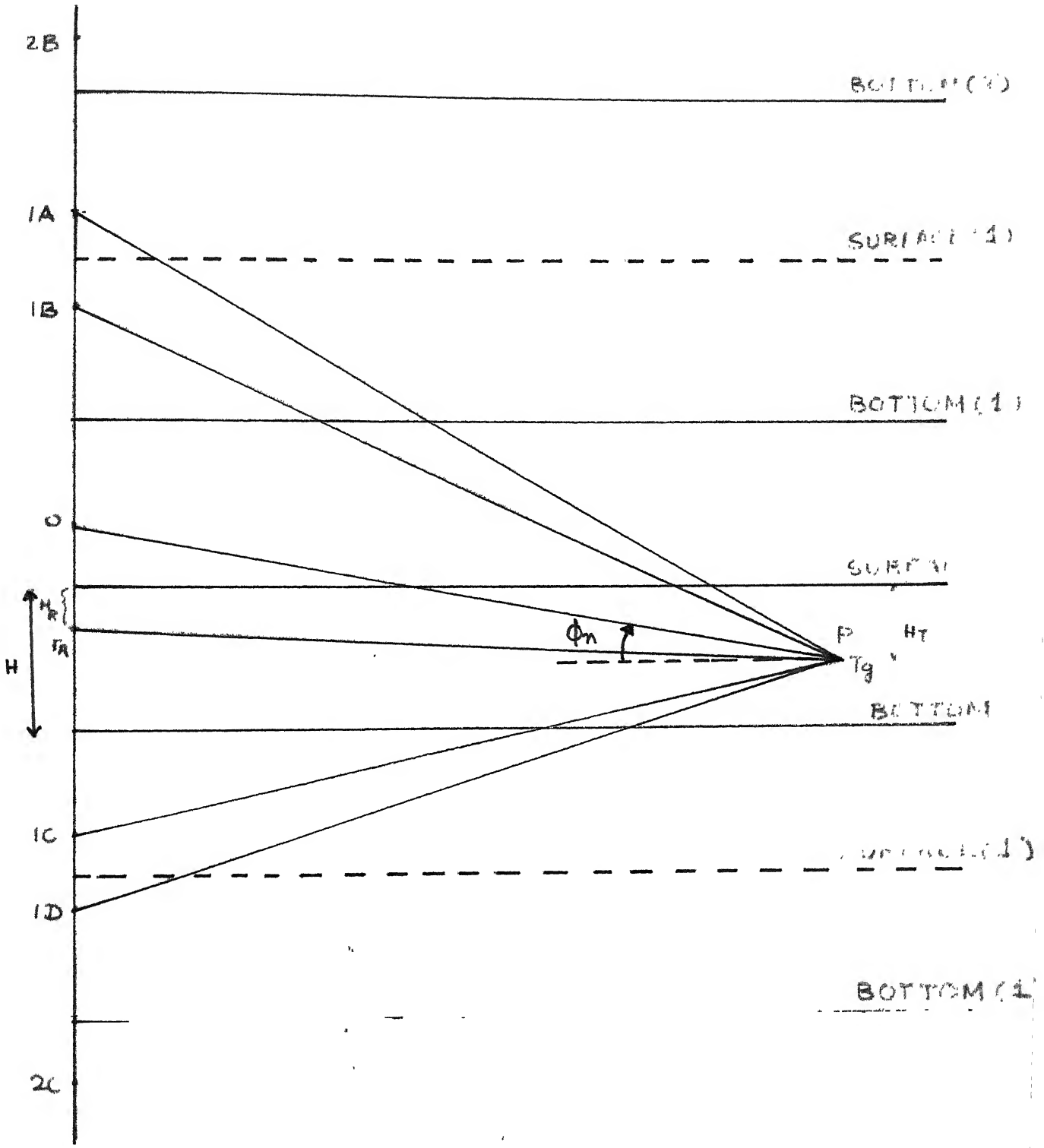

FIG. 2.11 : SOURCE AND IMAGES OF A [illegible] CHANNEL

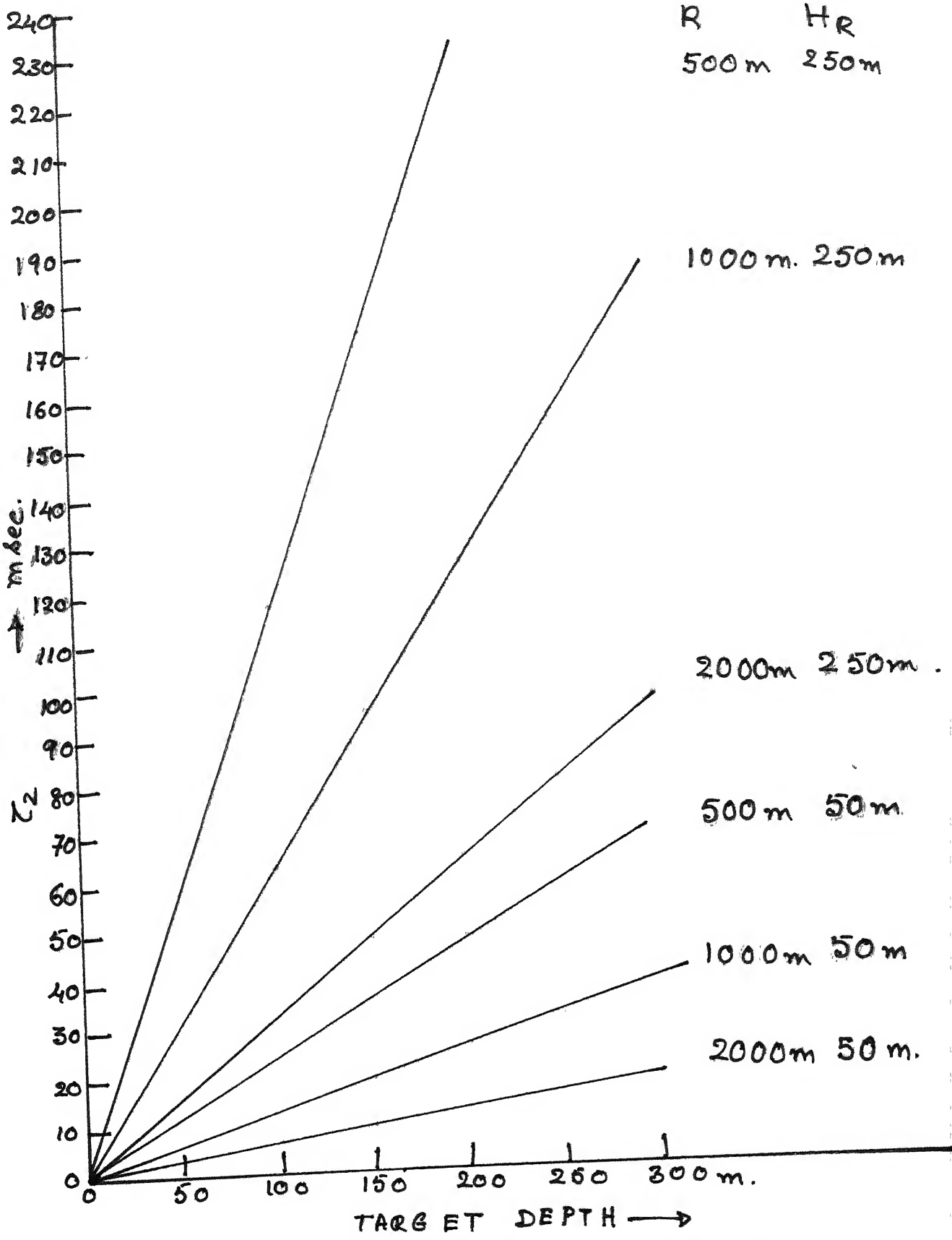

Graph 2.1 Time delay difference Vs H_T for τ_2

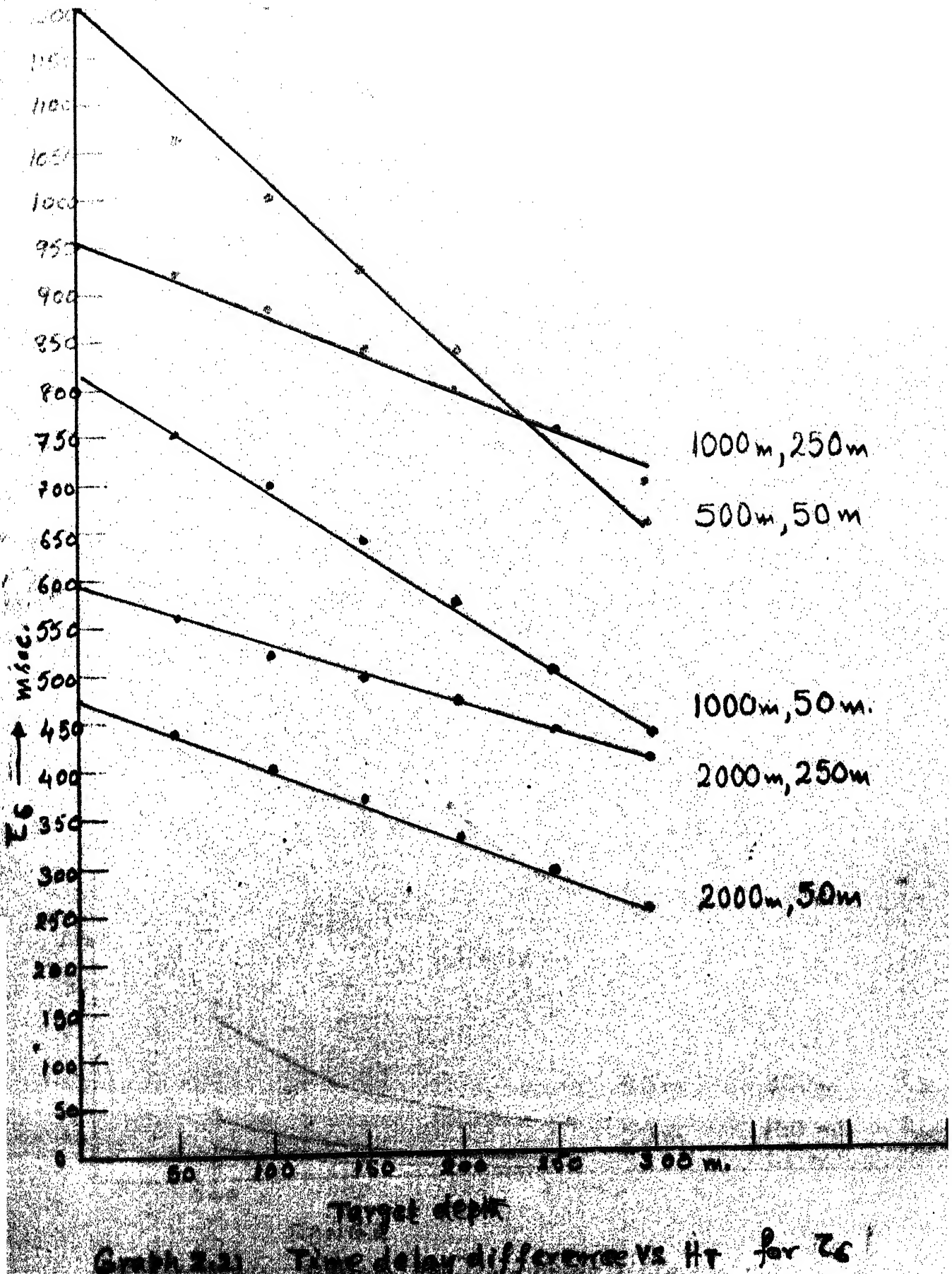

Graph 2.2: Time delay difference Vs Ht for Tc

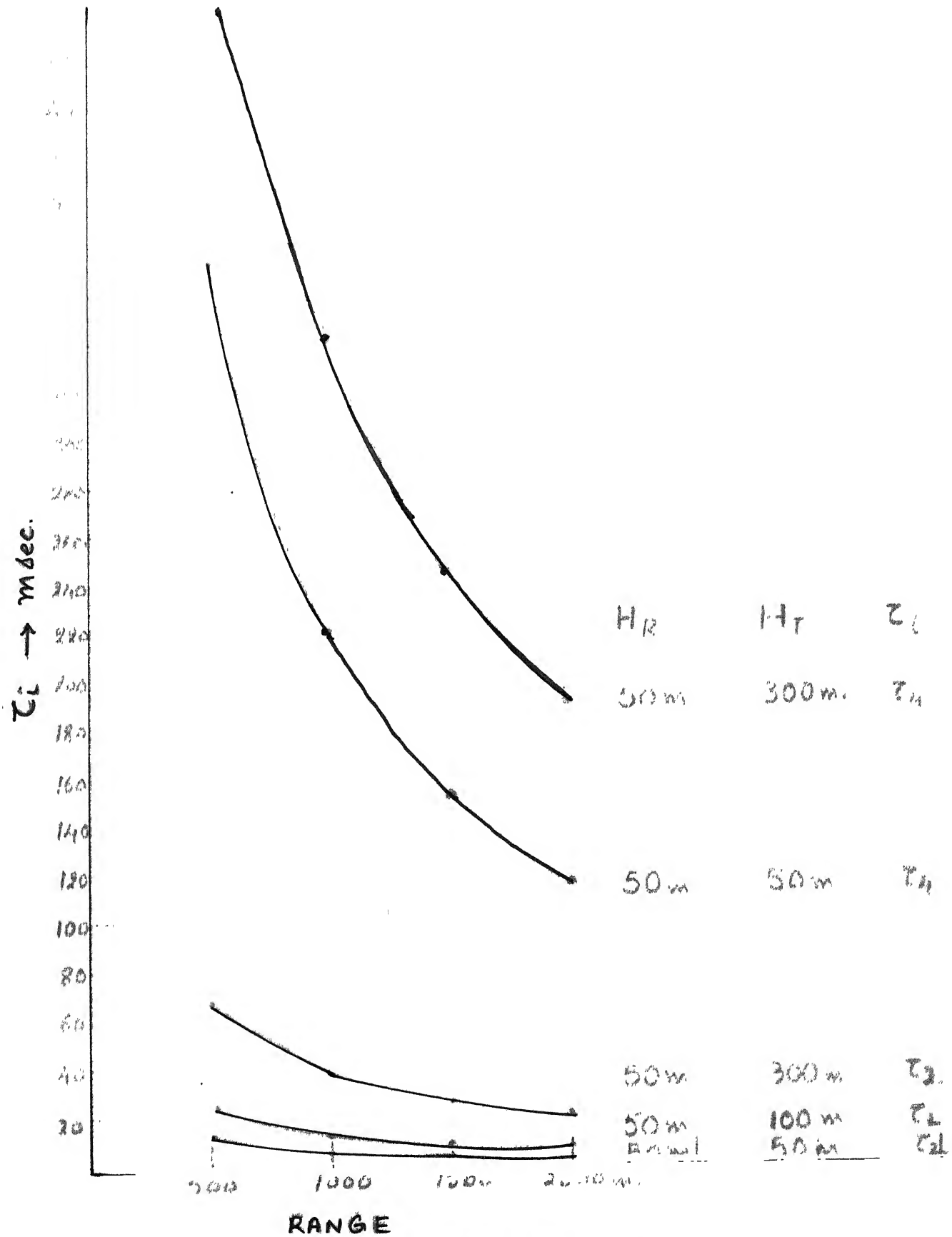

Graph 2·3 : Range Vs Time delay difference.

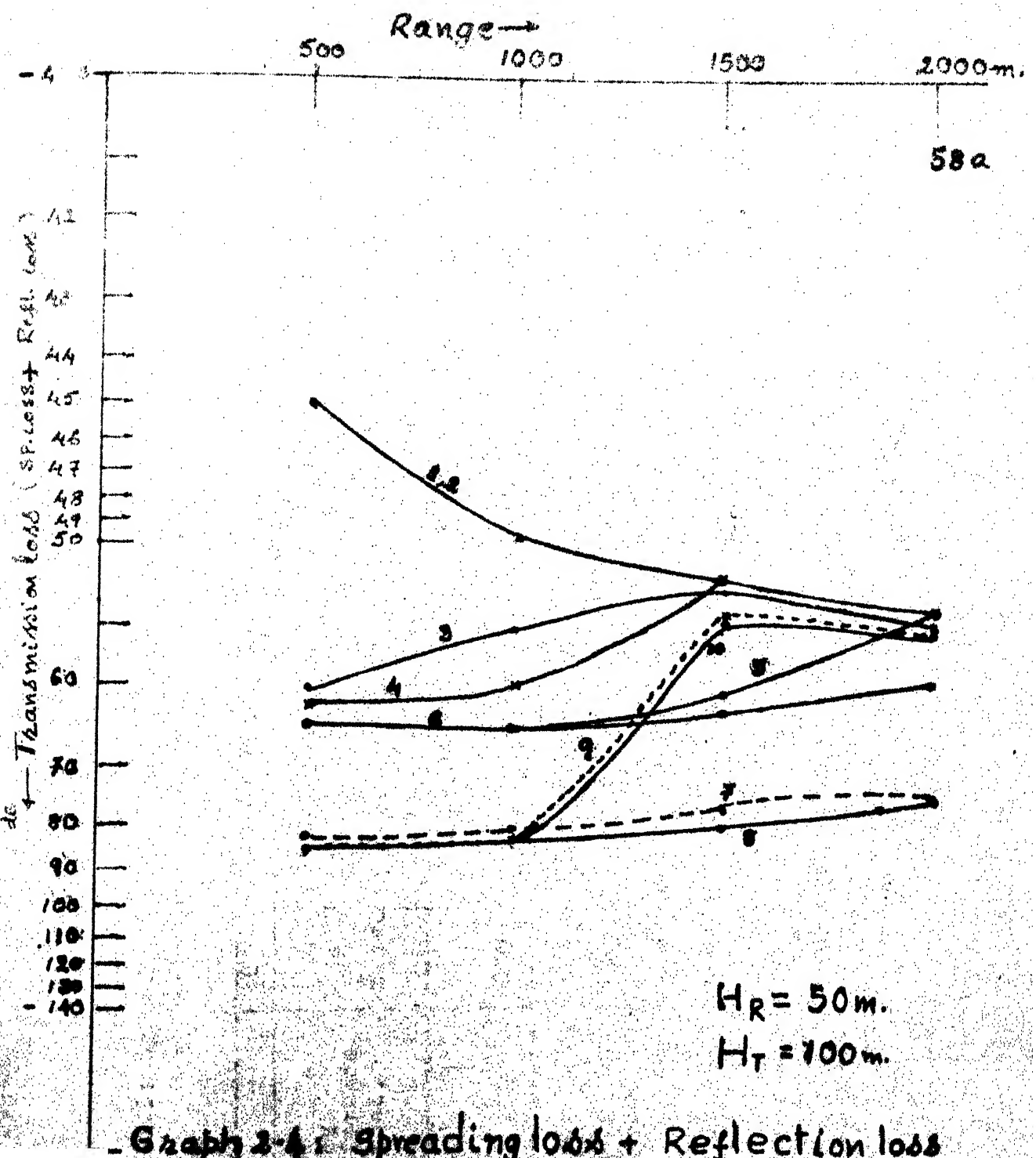

$H_R = 50$ m.
$H_T = 100$ m.

Graph 2-4 : Spreading loss + Reflection loss of various rays with respective range (Ref. also fig. 2.6)

Table 2.1: Spreads of time delay differences for rays 0,1,2 with respect to direct ray time delay.

Order n	0	1				2			
Time delay difference in msec. Range	2 m sec	3 msec	4 msec	5 msec	6 msec	7 msec	8 msec	9 msec	10 msec
50C Min.	0	0	0	0	420	420	550	550	1175
Max	320	320	530	530	1000	1000	1125	1125	1750
1000m Min	0	0	0	0	250	250	440	440	800
Max	190	190	350	350	700	700	950	950	1350
1500m Min	0	0	0	0	180	180	320	320	600
Max	130	130	250	250	520	520	740	740	1070
2000m Min	0	0	0	0	140	140	250	250	470
Max	100	100	190	190	400	400	600	600	880

Order '0' : Surface reflected ray
'1' : Rays with one bottom reflection
'2' : Rays with two bottom reflections

(Type of rays are shown in Fig. 2.6)

Table 2.2: Total number of arrivals and their distribution with respect to direct ray arrival time for different ranges.

Range (R)	Vertical height (h)	Total arrivals	Arrivals with respect range bin				
			1	2	3	4	5
500 m	< 50m	2	2	-	-	-	-
	≥ 50m	2	2	-	-	-	-
1000 m	< 50m	4	2	2	-	-	-
	≥ 50m	4	2	2	-	-	-
1500 m	< 50m	6	3	2	1	-	-
	≥ 50m	6	4	1	1	-	-
2000m	0 m	7	3	3	-	-	-
	50m	8	4	2	-	1	-
	100m	8	4	2	-	2	-
	150m	8	4	1	2	1	-
	200m	8	4	1	3	-	-

(h) : Vertical height between source/receiver and target depths.

Table 2.3: The type of rays that contribute at each range.

Range (R)	Vertical height (h)	Rays that contribute at receiver (Ref. Fig. 2.6)
500 m	0 - 250 m	1, 2, 3
1000 m	< 250 m	1, 2, 3, 4
	250 m	1, 2, 3, 5
1500 m	< 250 m	1, 2, 3, 4, 5, 6
	250 m	1, 2, 3, 4, 5, 7
2000 m	0 - 250 m	1, 2, 3, 4, 5, 7, 9

(h) : Vertical height between source/receiver and target depths.

CHAPTER 3

RECEIVERS FOR TARGET DETECTION

3.1 PROBLEM FORMULATION:

In Chapter 2, it was seen that the signal received from a shallow water target is a weighted sum of a finite number of replicas of the transmitted waveform with different delays and a common doppler shift. The number of paths that contribute significant energy at the receiver are limited by i) the beam patterns of the receiver and the transmitter and ii) the number of bottom reflections a ray path undergoes before it reaches the receiver.

In this chapter different receiver structures are considered and their relative performances studied. All the receivers are aimed at the detection of a target under the usual binary hypotheses testing [16].

Let the transmitted signal be a rectangular pulse with carrier frequency ω_o. Accordingly

$$S_T(t) = \sqrt{2}\, \mathrm{Re}[\sqrt{E_t}\, \tilde{f}(t)\, \exp(j\omega_o t)] \qquad (3.1)$$

where

$$\tilde{f}(t) = \frac{1}{\sqrt{T}} \quad 0 \leq t \leq T$$

$$= 0 \quad \text{otherwise} \qquad (3.2)$$

E_t is the transmitted signal energy and the complex envelope $f(t)$ has unity energy. Following our discussion in Chapter 2, we write the received signal component arriving via the ith path as

$$\gamma_{is}(t) = \sqrt{2}\ \mathrm{Re}\ [\sqrt{E_t}\,|a_i|\,f(t-2T_i)\exp j(-2\omega_o T_i+S_i)]e^{j(\omega_o+\omega_D)t} \tag{3.3}$$

where,

a_i is the attenuation suffered by the ray along the ith path,

T_i is one way travel time,

S_i is the phase introduced due to reflections at boundaries and target,

and ω_D is the doppler frequency.

The composite received signal may be written as;

$$\gamma(t) = \sqrt{2}\ \mathrm{Re}\ [\sqrt{E_t}\ \sum_i^M |a_i| f(t-2T_i)\exp j(-2\omega_o T_i+S_i)]e^{j(\omega_o+\omega_D)t} \tag{3.4}$$

where M is the number of significant paths. a_i's are modelled as complex Gaussian random variables. Each of these constitutes two parts. A complex deterministic variable a_{1i}, describes path losses and boundary losses. And a_{2i}, a

zero mean complex Gaussian random variable, describes the reflection coefficient of the target, which we assume to be a slowly fluctuating point target. a_{2i} has variance $2\sigma^2_{a_{2i}}$ and the phase S_i is uniformly distributed over $[0,2\pi]$.

Now we write

$$a_i = \tilde{a}_{1i} \cdot a_{2i}$$
$$= |\dot{a}_{1i}| \, |a_{2i}| \exp(j S_i)$$

Therefore the variance of a_i is given as

$$2\sigma^2_{a_i} = 2|\dot{a}_{1i}|^2 \sigma^2_{a_{2i}} \qquad (3.5)$$

The phase distribution of a_i is seen to be uniformly distributed with a bias component which is equal to a_{1i}'s phase. We also note $|\dot{a}_{2i}|$ is a function of target's aspect and altitude angles with respect to receiver; which inturn depend on path inclination angles θ_i. Hence $\tilde{a}_i$ have in general unequal variances.

We now consider the time delay (T_i) and attenuation coefficients ($\dot{a}_i$) normalized with respect to direct ray's time delay (T_d) and attenuation coefficient ($\dot{a}_d$). That is define

$$\tau_i \triangleq 2\,(T_i - T_d) \tag{3.6}$$

and $$b_i \triangleq \frac{a_i}{\sqrt{2\sigma_{ad}^2}} \tag{3.7}$$

for i=1... M.

τ_i's are now time delay differences and b_i's are normalized attenuation coefficients. If direct ray subscript is taken as '1', then $\tau_1 = 0$ and $2\sigma_{b_1}^2 = 1$.

Rewriting the composite received signal along with noise component which is considered to be a sample function from a zeromean complex white Gaussian random process, we have

$$\gamma(t) = \sqrt{2}\,\mathrm{Re}\left[\left\{\sqrt{E_t}\,\Sigma_i\, b_i\, f(t-\tau_i)\right\} \exp^{j}(\omega_o+\omega_D)t\right]$$

$$+\sqrt{2}\,\mathrm{Re}\,[\,w(t)\,\exp(j\omega_o t)] \tag{3.8}$$

As we observed in Section 2.6, the composite return signal is having a common doppler shift. Therefore with no loss of generality we equate ω_d to zero.

The complex envelope of the received signal is obtained under binary hypotheses testing as;

$$\gamma(t) = \Sigma_{i=1}^{M} \sqrt{E_t}\, b_i\, f(t-\tau_i) + w(t) : H_1$$
$$w(t) : H_0$$

where $0 < t < T' \triangleq T + \text{Max}(\ _j)\ ;\ j\ \ [1...M]$

and $E[\dot{w}(t)\ \dot{w}(u)] = 2\sigma_{\omega^2}\ \delta\ (t - u)$

We now consider various receiver configurations and attempt to evaluate their performances.

3.2 OPTIMUM RECEIVER:

The complex envelope of the received signal is given by equation (3.9) and is reproduced as

$$\dot{\gamma}(t) = \Sigma_i\ \sqrt{E_t}\ \dot{b}_i\ \dot{f}(t-\tau_i) + \dot{w}(t):\ H_1$$
$$\dot{w}(t):\ H_0$$

where attenuation coefficients ($\dot{b}_i$) are modelled as complex Gaussian random variables. Time delay differences (τ_i) are functions of target range, target depth and source depth. Hence τ_i's can be seen to be some functions of target depth if range and source depth are known. Since target may lie at any depth in the channel, τ_i may be modelled as random variables, in a range $\Delta_i\ \Delta\tau_{imax} - \tau_{imin}$.

Now we are interested in designing an optimum processor with above specifications, i.e., the problem is to observe $\dot{\gamma}(t)$ over an interval $[0,T']$ and decide whether H_0 or H_1 is true. The criterion may be either Bayes or Neyman-Pearson criteria.

Our observation is a time continuous random waveform. The first step is to reduce it to a set of random variables.

We observe in equation (3.9) that the received signal $\gamma(t)$ is a zeromean random process, with variance $K_{\gamma}(t,u)$ given by

$$K_{\gamma}(t,u) = E_t \Sigma_i 2\sigma_{b_i} E[f(t-\tau_i) f(u-\tau_i)] + 2\sigma_{\omega}^2 \delta(t-u) \tag{3.10}$$

We want to expand $\gamma(t)$ by using K.L. expansion method to obtain a set of uncorrelated random variables.

We write

$$\gamma(t) = \underset{N \to \infty}{\text{l.i.m.}} \Sigma_{i=1}^{N} \gamma_i \phi_i(t) \tag{3.11}$$

where $\gamma_i = \int_0^T \gamma(t) \phi_i^*(t)\, dt$

and $\{\phi_i(t)\}$ is a set of complete orthonormal functions. Expanding $\gamma(t)$ by using the above functions we will have

$$\gamma_i = \Sigma_j \sqrt{E_t}\, \rho_{ij} + w_i : H_1 \tag{3.12}$$

where $\rho_{ij} = \int_0^{T'} f(t-\tau_j) \phi_i(t) dt.$ (3.13)

and $w_i = \int_0^{T'} w(t) \phi_i(t)\, dt$ (3.14)

$\phi_i(t)$; i = 1,2,...N, has to satisfy the following integral equation:

$$\lambda_i \phi_i(t) = \int_0^T K_\gamma (t,u) \phi_i(u) du$$

where λ_i are eigen values.

The above integral equation may be written as;

$$\lambda_i \phi_i(t) = E_t \Sigma_j [2 \sigma_{b_j}^2 E[\int_0^{T'} f(t-\tau_j) f^*(u-\tau_j)]] \times \phi_i(u) du + 2\sigma_\omega^2 .$$

Instead of solving the above difficult integral equation with a Kernal involving the statistics of the various delays, τ_i, we explore the following alternative approach.

Towards that end consider the expansion of $\gamma(t)$ in terms of complete orthonormal set of functions $\{\psi_i(t)\}$, the first M of which are given by $f(t-\bar{\tau}_i)$ for some suitably chosen set of values $\bar{\tau}_i$; i = 1...M.

We define, now, two vector functions as follows:

$$\bar{F}(t) \triangleq [f(t-\tau_1) \; f(t-\tau_2) \; \ldots \; f(t-\tau_M)]^T \qquad (3.15)$$

$$\bar{F}(t) \triangleq [f(t-\bar{\tau}_1) \; f(t-\bar{\tau}_2) \; \ldots \; f(t-\bar{\tau}_M)]^T \qquad (3.16)$$

Then we expand $\gamma(t)$ over $\bar{F}(t)$ and the functions $\{\psi_i(t)\}_{M+1}^{\infty}$. We obtain a set of random variables γ_i,

$$\tilde{\gamma}_i = \int_0^{T'} \tilde{\gamma}(t)\, \tilde{f}^*(t-\bar{\tau}_i)dt$$

$$= \Sigma_j \sqrt{E_t}\, b_j \rho_j(i) + w_i \;:\; H_1$$
$$\tilde{w}_i \;:\; H_0 \qquad (3.17)$$

where $$\rho_j(i) = \int_0^{T'} f(t-\tau_j)\, \tilde{f}^*(t-\bar{\tau}_i)dt \qquad (3.18)$$

and $$\tilde{w}_i = \int_0^{T'} \tilde{w}(t)\, \tilde{f}^*(t-\bar{\tau}_i)dt \qquad (3.19)$$

For $i = M+1, \ldots$; $\tilde{\gamma}_i$ are same for both the hypotheses and provides no additional information and hence can be ignored. Observe that $\tilde{w}_i$ are uncorrelated random variables. The cross covariance of γ_i and $\tilde{\gamma}_K$ are given as

$$E[\tilde{\gamma}_i\, \gamma_K^*] = \Sigma_j\, 2\sigma_{b_j}^2\, E[\rho_j(i)\rho_j(K)] + 2\sigma_\omega^2 \quad iK \qquad (3.20)$$

Now we have a set of random variables $\tilde{\gamma}_i$, which are functions parameters b_j and $\rho_j(i)$. We want to now formulate the problem as a composite hypotheses problem. We first introduce some notation. Let

$$R \triangleq [\tilde{\gamma}_1, \tilde{\gamma}_2 \cdots \tilde{\gamma}_M]^T \qquad (3.21)$$

$$B \triangleq [b_1, b_2 \cdots b_M]^T \qquad (3.22)$$

$$\tilde{W} \triangleq [\tilde{w}_1, \tilde{w}_2 \cdots \tilde{w}_M]^T \qquad (3.23)$$

Accordingly we will have

$$E[B] = 0$$

$$\text{and } E[\tilde{B}\ B^{+}] = \tilde{\Lambda}_{\tilde{b}} \tag{3.24}$$

where $\tilde{\Lambda}_{\tilde{b}}$ is a diagonal matrix with diagonal elements equal to $2\sigma_{b_i}^2$.

We also define the correlation matrix,

$$P \triangleq \int_0^{T'} \tilde{F}(t)\ \bar{F}^{+}(t)\ dt \tag{3.25}$$

where $\rho_j(i) = \int_0^{T'} f(t-\tau_j)\ f^{*}(t-\bar{\tau}_i)dt$

The composite hypotheses problem is now to compute

$$\Lambda(\tilde{R}) = \frac{\int_{\tilde{B},\ P} p(R/B,\ P,\ H_1)p(\tilde{B})\ p(P)\ d\ B d\ P}{p\ (R\ /H_0)} \tag{3.26}$$

Towards evaluating $\Lambda(\tilde{R})$, we first consider evaluating $\Lambda(R/P)$ by averaging $\Lambda(\tilde{R}/\tilde{B}, P)$ over the space of B parameters. $\Lambda(\tilde{R}/P)$ is a complex Gaussian vector under both H_0 and H_1 and hence its solution is obtained by computing the conditional likelihood ratio, which is given in general as

$$\Lambda(\tilde{R}/P) = \frac{(\tilde{K}_o)^{1/2} \exp[-\frac{1}{2}(\tilde{R}^+ - M_1^+)\, Q_1 (\tilde{R} - \tilde{M}_1)}{(K_1)^{1/2} \exp[-\frac{1}{2}(\tilde{R}^+ - \tilde{M}_o)\, Q_o\, (R - M_o)]} \tag{3.27}$$

where,

$$E[\tilde{R}/H_1] = M_1 ; E[\tilde{R}/H_o] = \tilde{M}_o$$

$$E[(\tilde{R} - M_1)(\tilde{R}^+ - M_1^+)/H_1] = K_1$$

$$E[(\tilde{R} - \tilde{M}_o)\,(R^+ - \tilde{M}_o^+)/H_o] = \tilde{K}_o$$

$$\tilde{Q}_1 = K_1^{-1} ; \quad Q_o = \tilde{K}_o^{-1}.$$

In the present problem, we have

$$\tilde{R} = \sqrt{E_t}\; P^T B + \tilde{W} : H_1$$

$$= \tilde{W} : H_o \tag{3.28}$$

and $\tilde{M}_1 = \tilde{M}_o = 0$

$$\tilde{K}_1 = E_t\; P^T \Lambda_b\, P + \tilde{K}_W \tag{3.29}$$

$$\tilde{K}_o = \tilde{K}_W = 2\sigma_\omega^2\, I \tag{3.30}$$

Then the conditional likelihood ratio is simplified to

$$\Lambda(\tilde{R}/P) = \left|\frac{\tilde{K}_W}{\tilde{K}_1}\right|^{1/2} \exp[\tfrac{1}{2}\tilde{R}^+ (\tilde{Q}_o - Q_1)\tilde{R}] \tag{3.31}$$

Now we need to compute $\tilde{Q}_o - \tilde{Q}_1$ to obtain a simple structure for the above ratio.

Consider the signal component of covariance matrix $\tilde{K}_1$, and it is given as

$$\tilde{K}_{1S} \triangleq E_t \, P^T \Lambda_b \, P \tag{3.32}$$

This is a non-diagonal matrix implying that the components of vector $\tilde{R}$ are not independent. We now diagonalize the matrix $\tilde{K}_{1S}$ by solving its characteristic equation and obtain the eigen values and eigen vectors. If $\tilde{K}_{1S}$ is not positive definite, we augment the eigen vectors with some more to form a complete set. We have seen K_W to be a diagonal matrix with equal diagonal elements $(2\sigma_\omega^2)$ and so the diagonalizing matrix $(\tilde{\Phi})$ will not effect the matrix $\tilde{K}_W$. So write

$$\tilde{K}'_{1S} = \tilde{\Phi} \, K_{1S} \, \tilde{\Phi}^+$$

$$\text{and} \quad \tilde{K}'_1 = \tilde{K}'_{1S} + \tilde{K}_W \tag{3.33}$$

If $2\sigma^2$ are the diagonal elements or eigen values of $\tilde{K}'_{1S}$, they represent the energy components of received signal along different basis functions and also their sum is always constant irrespective of the choice of $\tilde{\Phi}$. Now $\tilde{Q}_1' - \tilde{Q}_o'$ is obtained as

$$\check{Q}_1 - \check{Q}_0' = \begin{bmatrix} \frac{\sigma_1^2}{\sigma_\omega^2(\sigma_1^2+\sigma_\omega^2)} & & 0 \\ & \ddots & \\ 0 & & \frac{\sigma_M^2}{\sigma_\omega^2(\sigma_M^2+\sigma_\omega^2)} \end{bmatrix} \tag{3.34}$$

Substituting the above matrix in conditional likelihood ratio, we obtain,

$$\Lambda(\check{R}'/P) = \prod_i \left[\frac{\sigma_\omega^2}{\sigma_i^2+\sigma_\omega^2}\right]^{1/2} \exp \frac{1}{2\sigma_\omega^2} \sum_i \frac{\sigma_i^2}{\sigma_i^2+\sigma_\omega^2} \check{Y}_i'^2 \tag{3.35}$$

where $\check{R}' = \check{\phi}^+ \check{R}$ (3.36)

The above ratio is developed with apriori knowledge of P i.e., $P_j(i)$ for $i_{i,j}$= 1...M. Now if we have the probabilistic knowledge of P, then the optimum processor would be

$$(\check{R}') = \int_P (\check{R}'/P)\, p(P)\, dP \tag{3.37}$$

This integration in general will be difficult and we consider a case where M = 2.

Example: M = 2:

$$\underline{R} = [\, \gamma_1, \gamma_2 \,]^T$$

where $\gamma_i = \int_0^{T'} \gamma(t)\, f^*(t-\tau_1)dt$

we have

$$\gamma_1 = \sqrt{E_t}\,(\rho_1(1)\, b_1 + \rho_2(1)\, b_2) + w_1$$

$$\gamma_2 = \sqrt{E_t}\,(\rho_2(1)\, b_1 + \rho_2(2)\, b_2) + w_2$$

where $\rho_j(i) = \int_0^{T'} f(t-\tau_j)\, f^*(t-\tau_i)dt$

Then define $K_1 \triangleq \begin{bmatrix} K_{11S} & K_{12S} \\ K_{21S} & K_{22S} \end{bmatrix} + 2\sigma_\omega^2 \begin{bmatrix} 1 & 0 \\ 0 & 1 \end{bmatrix}$

where $K_{11S} \triangleq A \triangleq E_t(\sigma_{b_1}^2\, \rho_1^2(1) + \sigma_{b_2}^2\, \rho_2^2(1))$

$$K_{22S} \triangleq B \triangleq E_t(\sigma_{b_1}^2 \rho_1^2(2) + \sigma_{b_2}^2 \rho_2^2(2)\,.$$

and $K_{21S} = K_{12S} \triangleq C \triangleq E_t(\sigma_{b_1}^2\, \rho_1(1)\rho_1(2) + \sigma_{b_2}^2 \rho_2(2))$

Solving the characteristic equation we will have

$$\lambda_1 = A + \frac{c^2}{A-B} \text{ and } \lambda_2 = B - \frac{c^2}{A-B}$$

if $c^2 < (A-B)^2/4$.

then the conditional likelihood ratio is given as

$$\Lambda(R'/P) = \frac{\sigma_\omega^2}{1\ 2} \exp\left[\frac{1}{2\sigma_\omega^2}\left\{\frac{1}{1+\sigma_\omega^2}\ \gamma_1'^2 + \frac{2}{2+\sigma_\omega^2}\right\}\right]$$

and then

$$\Lambda(R') = \int \Lambda(R'/P)\ p(P)\ dP, \qquad (3.37a)$$

where $\rho_j(i) = \int_0^T f(t-\tau_i)\ f^*(t-\overline{\tau}_i)dt.$

Now $\rho_j(i)$ is a random variable and it's probability density depends on the density of τ_j. From $\rho_j(i)$ we now have to compute joint densities λ_1 and λ_2 to evaluate the integral (3.37a).

This approach of evaluating likelihood ratio involves extensive computation and the receiver implementation would also be difficult; even for the case M = 2.

But however, if we could compute the joint densities of λ_1 and λ_2 and assume high signal to noise ratios, we may be able to obtain a simpler structure. The eigen values λ_1 and λ_2 are the received signal energy components and if $\lambda_i >> \sigma_\omega^2$, in equation (3.35), we see that

$$\Lambda(R') = 2\alpha\ \sigma_\omega^2 \exp\left[\frac{1}{2\sigma_\omega^2}\right]\left(\gamma_1'^2 + \gamma_2'^2\right)] \gtrless \eta \qquad (3.38)$$

where

$$\alpha \quad \iint \frac{1}{\lambda_1 \lambda_2} \; p(\lambda_1 \lambda_2) d\lambda_1 \; d\lambda_2 \qquad (3.39)$$

Likelihood ratio is obtained as,

$$\ell(R') = \sum_{i=1}^{M=2} \gamma_i'^2 \underset{H_0}{\overset{H_1}{\gtrless}} \gamma^*$$

The performance of this receiver can be easily obtained as $\ell(R')$ is having central chi-square distribution.

We can also observe that for high order M, the sufficient statistic is still same i.e.,

$$\ell(R') = \sum_{i=1}^{M} \gamma_i'^2 \gtrless \gamma^*$$

if high SNR condition is satisfied. But we need to compute Mth order joint density function and then evaluate the corresponding integral.

For low signal to noise ratios, the receiver may not be as simple as shown above. By appropriate modelling of densities of τ_i, we may still be able to realize the optimum processor.

We now consider some other receivers wherein we have precise information of the time delay parameters.

3.3 OPTIMUM RECEIVER WHEN TIME DELAYS ARE PERFECTLY KNOWN:

In Section 3.2 we have seen an optimum receiver formulation when B and P are random vectors and matrices respectively. This was found to be a difficult problem even for M=2. Now we consider an optimum processor for the situation in which time delays τ_j and therefore P are perfectly known. The performance of this receiver if evaluated gives a bound on the performance of the receiver discussed in Section 3.2. In Section 3.4 when we discuss a conventional receiver with perfectly known delays, the performance of the optimum receiver will give us an estimate of the degradation that will occur with a conventional receiver.

We as seen in Section 3.2, again consider a set of orthonormal functions $\{\psi_i(t)\}$ of which the first M functions will be F(t) (eqn. (3.15). This choice of F(t) is essential to obtain uncorrelated noise components when $\gamma(t)$ is expanded. Under known P, γ_i are zeromean Gaussian under both the hypotheses, but K_1 will be non-diagonal. Solution of it's characteristic equation gives a transformation matrix which diagonalizes the kernal of R under H_1. Now we obtain the new vector components of R R' and the log-likelihood ratio will be

$$\ell(R') = \Sigma_i \frac{\sigma_i^2}{\sigma_i^2+\sigma_\omega^2} \gamma_i'^2 \qquad (3.40)$$

This is to be compared against a threshold γ^* where

$$\gamma^* = \left\{ \ln\eta + \Sigma_i \ln \frac{\sigma_i^2+\sigma_\omega^2}{\sigma_\omega^2} \right\} \frac{2\sigma_\omega^2}{} \qquad (3.41)$$

The receiver may be implemented as shown in Fig. 3.1.

3.3.1 Performance Evaluation:

In the hypotheses testing problems we know that the log-likelihood ratio is given by $\ell(R)$ and is compared against a threshold for detection of target. $\ell(R)$ is a random variable and it's density depends on the hypotheses considered. If the densities of $\ell(R)$ are known under H_o and H_1 in a binary hypotheses problem; we can compute the false alarm and probability of miss obtained for a given threshold and signal to noise energy.

As seen in eqn. (3.40), the random variable $\ell(R)$ is a sum of squares M Gaussian random variables with unequal weights.

The computation of $p_{/H_1}(L/H_1)$ is a difficult job as it involves unequal weights for the variables. Therefore we compute the performance bounds for the above receiver through moment generating functions [17]. These bounds are called chernoff's bounds.

These bounds are found by computing a function $\mu(s)$ given as,

$$\mu(s) = \ln \int_{-\infty}^{\infty} [p_{\gamma/H_1}(R/H_1)]^s [p_{\gamma/H_o}(R/H_o)]^{1-s} dR \qquad (3.42)$$

where 's' is taken as a parameter such that $s \geq o$. Then false alarm is given as [17],

$$P_F \leq \text{Exp}\left[(\mu/s) - s\,\mu(s) + \frac{s^2}{2}\,\mu(s))\,\text{erfc}^*(s\sqrt{\mu(s)})\right] s \geq o \qquad (3.43)$$

and probability of miss is given by

$$P_M \quad \exp(\mu(s) - (1-s)\,\mu(s) + \frac{(1-s)^2}{2}\,\mu(s))\,\text{erfc}^*((1-s)\sqrt{\mu(s)}) \qquad s \leq 1 \qquad (3.44)$$

where $\mu(s)$ and $\mu(s)$ are the first and second derivatives of $\mu(s)$.

The minimum bound is obtained by computing s_{min}, given as,

$$\mu(s)\Big|_{s=s_{min}} = \eta \qquad (3.45)$$

where η is the threshold. For equal probability of occurrance and equal cost functions, we have $\eta = 0$.

Computing a s_{min} satisfying the above equation, now false alarm and probability of miss are given as;

$$P_F \leq \text{Exp}\left[\mu(s) + \frac{s^2}{2}\ddot{\mu}(s)\right]\text{erfc}^*(s\sqrt{\ddot{\mu}(s)})\Big|_{s=s_{min}} \quad (3.46)$$

$$P_M \leq \text{Exp}\left[\mu(s) + \frac{(1-s)^2}{2}\ddot{\mu}(s)\right]\text{erfc}^*(s\sqrt{\ddot{\mu}(s)})\Big|_{s=s_{min}} \quad (3.47)$$

where $0 \leq s \leq 1$.

If $s_{min}\sqrt{\ddot{\mu}(s_{min})} > 3$, then

$$\text{erfc}^*\left(s_{min}\sqrt{\ddot{\mu}(s_{min})}\right) \frac{1}{\sqrt{2\pi}\, s_{min}\sqrt{\ddot{\mu}(s_{min})}} e^{-s_{min}^2/2}\dot{\mu}(s_{min})$$

Similarly if $(1-s_{min})\sqrt{\ddot{\mu}(s_{min})} > 3$ then,

$$\text{erfc}^*\left((1-s)\sqrt{\ddot{\mu}(s)}\right)\Big|_{s=s_{min}} \frac{\exp\left(\frac{(1-s)^2}{2}\ddot{\mu}(s)\right)}{\sqrt{2\pi}(1-s)\sqrt{\ddot{\mu}(s)}}\Big|_{s=s_{min}}$$

Therefore,

$$P_F \leq \frac{1}{\sqrt{2\pi s^2\ddot{\mu}(s)}} \exp\left[\mu(s)\right]\Big|_{s=s_{min}} \quad (3.48)$$

$$P_M \leq \frac{1}{\sqrt{2\pi(1-s)^2\ddot{\mu}(s)}} \exp\left[\mu(s)\right]\Big|_{s=s_{min}} \quad (3.49)$$

3.3.2 To Compute Performance Bounds for Equation (3.40):

We have seen in Section 3.3.1 that $\mu(s)$ is given as

$$\mu(s) = \ln \int_{-\infty}^{\infty} [\Lambda(R')]^s \, p_{\gamma'/H_o}(R/H_o)dR'.$$

We know $\Lambda(R')$ and $p_{\gamma'}/H_o$ (R/H_o) where $\Lambda(R')$ is given by eqn. (3.39) where $Q_o' - Q_1'$ is given as

$$Q_o' - Q_1' = \begin{bmatrix} \frac{\sigma_1^2}{(\sigma_1^2+\sigma_\omega^2)\sigma_\omega^2} & & 0 \\ & \ddots & \\ 0 & & \frac{\sigma_M^2}{(\sigma_M^2+\sigma_\omega^2)\sigma_\omega^2} \end{bmatrix}$$

Then $\mu(s)$ can be evaluated and is seen equal to

$$\mu(s) = \ln \int_{-\infty}^{\infty} \left[\prod_{i=1}^{M} \left(\frac{\sigma_\omega^2}{\sigma_1^2+\sigma_\omega^2} \right) \right]^{s/2} \prod_{i=1}^{M} \left[\exp \left[\frac{s}{2} + \frac{\gamma_i'^2}{\sigma_\omega^2} - \frac{\gamma_i'^2}{\sigma_i^2+\sigma_\omega^2} \right] \right] \times \frac{1}{\sqrt{2\pi\sigma_n^2}} \exp\left[- \frac{\gamma_i'^2}{2\sigma_\omega^2} \right] d\gamma_i' \qquad (3.50)$$

Completing the squares in exponent and solving the integral $\mu(s)$ is simplified as,

$$\mu(s) = \Sigma \frac{1}{2} \ln \left[\frac{(\sigma_\omega^2)^s (\sigma_i^2+\sigma_\omega^2)^{1-s}}{(1-s)\sigma_i^2 + \sigma_\omega^2} \right]$$

Now to compute Chernoff's bounds, we proceed as follows:

i) Equation (3.50) is computed for various values of 's' in the interval [0,1].

ii) The minimum value of $\mu(s)$ is found and corresponding 's' is the s_{min} and at this 's' we have $\dot{\mu}(s) = 0$.

iii) We now compute $\ddot{\mu}(s)$ as

$$\ddot{\mu}(s) = \frac{1}{2} \Sigma_i \left[\frac{(\sigma_i^2/\sigma_\omega^2)}{(1+(1-s)\ \sigma_i^2/\sigma_\omega^2} \right]^2$$

iv) Calculate $\ddot{\mu}(s_{min})$.

v) Define $x \triangleq s_{min} \sqrt{\ddot{\mu}(s_{min})}$ and $y \triangleq (1-s_{min})\sqrt{\ddot{\mu}(s_{min})}$ now if erfc* (x) > 3, the false alarm is given by eqn. (3.48) or else by eqn. (3.46). Similarly if erfc*(y) > 3, the probability of miss is given by eqn. (3.45) or else by equation (3.47).

vi) The total probability of error is given by, under equal likely conditions, $P_r(\epsilon) = \frac{1}{2} P_F + \frac{1}{2} P_{MA}$.

The results on these bounds are discussed in Section 3.5. We now proceed to consider a much simpler processer called conventional receiver.

3.3.3 Selection of Transmitted Waveform to Reduce Receiver Complexity:

The complexity of the receiver structure considered in Section 3.3 arises from the fact that the signal contributions reaching the receiver via the various ray paths, are

not orthogonal. One way of making them orthogonal would be to choose a transmitted wave form f(t), such that its correlation function

$$R_f(\tau) \triangleq \int_0^T f(t)\, f^*(t+\tau)dt \qquad (3.51)$$

satisfies the property,

$$R_f(\tau) = 0 \qquad \text{for all } \tau \geq T_c$$

where,

$$T_c \leq \min_{\substack{i,j \\ i\neq j}} (|\tau_i - \tau_j|) \qquad (3.52)$$

It may be recalled that all τ_i, $i\neq j$, are non-negative differences in delays, between the reflected ray paths and the direct ray.

A linear frequency modulated waveform or a Barker coded sequence of pulses or a PRBS sequence, with appropriate choice of parameters will approximately satisfy the condition given in equation (3.52).

Assuming as in the previous section that the time delays τ_i are perfectly known at the receiver, with a transmitted waveform f(t) chosen as above, we can easily show the simplification that will occur in the receiver structure, compared to the receiver shown in Section 3.3. For this purpose

instead of considering the subset of the orthonormal functions $f(t-\tau_i)$; i=1...M as the first M members of the CON set $\{\psi_i(t)\}_{i=1}^{\infty}$ as in Section 3.2, we now choose them to be $f(t-\tau_i)$; i=1...M. With such a choice in view of equation (3.52), it is easily seen that

$$\rho_j(i) = \begin{cases} 1 & \text{if } j=i \\ 0 & \text{otherwise} \end{cases} \qquad (3.53)$$

As before the hypotheses testing problem simplifies to

$$\gamma_i = \Sigma_j \sqrt{E_t}\, b_j \rho_j(i) + w_i \quad : H_1$$
$$w_i \quad : H_0 \qquad (3.54)$$

The covariance matrix of the measurements is now a diagonal matrix with i,jth element given as

$$E[\gamma_i \gamma_j^*] = 2E_t \sigma_{b_i}^2 + 2\sigma_\omega^2 \delta_{ij}$$

Proceeding as in Section 3.2, the likelihood ratio is given as

$$\Lambda(R) = \prod_{i=1}^{M} \left[\frac{\sigma_\omega^2}{E_t\sigma_{b_i}^2+\sigma_\omega^2} \right] \exp \left[\Sigma_i \frac{E_t\sigma_{b_i}^2}{2\sigma_\omega^2(E_t\sigma_{b_i}^2+\sigma_\omega^2)} \cdot]|\gamma_i^2|\right] \qquad (3.55)$$

The log-likelihood ratio is;

$$\ell(R) = \Sigma_i \frac{E_t\, \sigma_{b_i}^2}{(E_t\sigma_{b_i}^2 + \sigma_\omega^2)} \; |\gamma_i|^2 \qquad (3.56)$$

and the threshold $\gamma^* = [\ln n - \ln \prod_{i=1}^{M} \frac{\sigma_\omega^2}{E_t\sigma_{b_i}^2 + \sigma_\omega^2}]2\sigma_\omega^2$

The receiver implementation is shown in Fig. 3.2.

The performance bounds of this receiver can be computed. This can be easily carried out with a substitution of $E_t\sigma_{b_i}^2/(E_t\sigma_{b_i}^2 + \sigma_\omega^2)$ in place of $\sigma_i^2/(\sigma_i^2+\sigma_\omega^2)$ in eqn. (3.50). Therefore $\bar{\mu}(s)$ is given as

$$\mu(s) = \frac{1}{2} \Sigma \ln \frac{(\sigma_\omega^2)^s (E_t\sigma_{b_i}^2 + \sigma_\omega^2)^{1-s}}{(1-s) E_t \sigma_{b_i}^2 + \sigma_\omega^2}$$

and

$$\mu(s) = \frac{1}{2} \Sigma \left[\frac{E_t \sigma_{b_i}^2 / \sigma_\omega^2}{1+(1-s)(E_t\sigma_{b_i}^2 / \sigma_\omega^2} \right]^2$$

We can compute Chernoff bounds by computing s_{min} and then substituting this in corresponding equations.

The results obtained by this method are discussed in Section 3.5.

3.4 CONVENTIONAL RECEIVER:

Consider the equation (3.9) in which we assumed b_i are zero mean complex Gaussian random variables. τ_i's, the time delay differences are assumed to be known. Depending on the values of τ_i and τ_j, we have $f(t-\tau_i)$ and $f(t-\tau_j)$ overlapping.

The conventional receiver is designed with the view that only direct ray and the white noise component are present. Then knowing the direct ray time delay (T_1), we compute

$$\gamma_1 = \int_0^T \gamma(t)\, f^*(t - T_1).dt \qquad (3.57)$$

or equivalently when we assume $\tau_1 = 0$, we have

$$\gamma_1 = \int_0^T \gamma(t)\, f^*(t)dt$$

$$= \Sigma_i \sqrt{E_t}\ b_i \rho_i(1) + \omega_i : H_1 \qquad (3.58)$$

$$\omega_1 : H_0$$

where,

$$\rho_i(1) = \int_0^T f(t - \tau_i)\, f^*(t - \tau_i)dt \qquad (3.59)$$

and $\rho_i(1)$ are known.

Therefore γ_1 is a sum of utmost independent zero mean complex Gaussian random variables along with a white noise sample, under H_1. Hence γ_1 is a complex Gaussian random variable under H_1 with zero mean and variance $2(\sigma_1^2+\sigma_\omega^2)$ where

$$\sigma_1^2 = \Sigma_i E_t \sigma_{b_i}^2 \rho_i^2(1) \qquad (3.60)$$

Under H_0, γ_1 is having variance $2\sigma_\omega^2$. Then likelihood ratio is;

$$\Lambda(R_1) = \frac{\sigma_n^2}{\sigma_1^2+\sigma_\omega^2} \exp\left[(\gamma_1)^2 \frac{\sigma_1^2}{\sigma_\omega^2(\sigma_1^2+\sigma_\omega^2)}\right] \gtrless \eta \tag{3.61}$$

and sufficient statistics is

$$\ell(R) = |\gamma_1|^2 \gtrless \gamma^* \tag{3.62}$$

where,

$$\gamma^* = \left[\ln\eta - \ln\frac{\sigma_\omega^2}{\sigma_1^2+\sigma_\omega^2}\right] \frac{\sigma_\omega^2(\sigma_1^2+\sigma_\omega^2)}{\sigma_1^2} \tag{3.63}$$

Performance of conventional receiver:

We have

$$\ell(R) = |R_1|^2 = \left|\int \gamma(t)\, f^*(t-\ )dt\right|^2 \tag{3.64}$$

and we know the receiver performance is given by,

$$\Delta = \frac{E[(R_1)^2/H_1 \cdot E[(R_1)^2/H_0]}{E[|R_1|^2/H_0]} \tag{3.65}$$

$$= \frac{\Sigma E_t \sigma_{b_i}^2 \ i^2(1)}{\sigma_\omega^2} \quad \text{from equation (3.60)}$$

Now we know that false alarm P_F and probability of detection P_D are related as;

$$P_F = (P_D)^{1+\Delta} \tag{3.66}$$

Now for various values of SNR, the performance of conventional receiver can be computed. In Section 3.5 we compare the performance of this receiver with the performance bounds obtained for the optimum receiver with known time delay differences τ_i, considered in Section 3.3.

3.5 PERFORMANCE CALCULATIONS OF CONVENTIONAL RECEIVER:

The performance of a conventional receiver can be evaluated from the plots of probability of detection (P_D) with respect to SNR for given values of probability of false alarm (P_F). The relation between P_F and P_D is given as (from equation (3.66);

$$P_F = (P_D)^{1+\Delta} \qquad (3.66)$$

where,

$$\Delta = \frac{E_t}{\sigma_\omega^2} \Sigma_i \sigma_i \sigma_{b_i}^2 \rho_i^2(1)$$

Here $\sigma_{b_i}^2$ is the variance of the reflection coefficient which also includes path and boundary losses. $\rho_i(1)$ is given as

$$\rho_i(1) = \int_0^T f(t-\tau_i) f^*(t-\tau_1)dt$$

We observe that $2E_t \sigma_{b_i}^2$ to be the total energy that arrives via ith path and therefore $2E_t \sigma_{b_i}^2 \rho_i^2(1)$ is the amount of

energy that ith path contributes in the performance factor 'Δ'. If E_t/σ_ω^2 is the signal to noise ratio, then $\Sigma_i \sigma_{b_i}^2 \rho_i^2(1)$ gives the multiplicating factor, which is the improvement in the amount of energy that arrives in range bin 1. This multiplicating factor, we call as multipath effect (M.E.). Therefore,

$$M.E. = \Sigma_i \sigma_{b_i}^2 \rho_i^2(1).$$

As we observe from equation (3.66), the magnitude of M.E. has direct bearing on ROC curves, computed for a receiver which receives only direct path. As M.E. $\geq$ 1 always in a multipath environment, the receiver performs better than the receiver which is operating in single path environment. Hence in the following we explore the characteristics of channel which effect M.E. and the performance of the receiver.

Define 'h' to be the vertical distance between source and target i.e., $h \triangleq H_R \sim H_T$ where H_R is source depth and H_T is the target depth.

The magnitude of M.E. varies with respect to range, source and target depths. We plotted various graphs depicting the variations of M.E. with the above parameters. We infer the following facts.

Graph 3.1: This graph is plotted for the variations in M.E. with respect to range for different h, with H_R = 150 m. If the source is located at the middle of the channel, the M.E. linearly increases with range irrespective of the target depth. But for a given range, the M.E. increases with h. At h = 0, the M.E. is minimum. This is due to less number of arrivals into first range bin (RB1) compared to h>0 (refer Table 3.1).

We observe that the number of arrivals in RB1 decides the initial value of M.E. and M.E. increases with range and this is because the net amount of overlap in RB1 by other rays, is increasing.

Graphs 3.2 to 3.3: This graph indicates the changes in M.E. with range, considering 'h' as a parameter, with H_R = 50, 250m. If h is a maximum, i.e., in a situation where source is close to one boundary and the target is close to another boundary, the M.E. is negligible at short ranges and has steep gradient with respect to range. We also observe, with a decrease in h the gradient also is reduced. For h equal to 200m, the increase in M.E. is 200% over a range of 1500m, and for h equal to zero, the increase is just 10% for the corresponding range. But it is seen that, for h=0 at short ranges, the M.E. is 70% higher than the M.E. at h=200m. These facts can be explained as follows.

For h = 200m, in Table 3.1 we observe that three new paths arrive in RB1 when target range changes from 500 to 1000m. This contributes to the steep gradient corresponding to this curve. Similar effect, but to a lesser extent is seen for other 'h' and hence their gradients are less. For h=200m; there are no new arrivals after 1000m, but because the net amount of overlap increases in RB1 with respect to range, the M.E. also increases. For h = 0 m., the net amount of overlap is not changing markedly and hence there is no relative improvement beyond 100m range. At range of 500m, the M.E. increases inversely proportional to h, because the amount of overlap of the two rays present in RB1 increases with respect to h. (Refer Section 2.6).

Graph 3.4, 3.5: This graph indicates the variations in M.E. with respect to target depth for a given H_R, taking range as varying parameters for different curves.

When the source is at the middle of the channel, then M.E. is almost constant with target depth irrespective range. These curves only show a small reduction in M.E. when h=0. This is due to number of arrivals at h=0 are less than number of arrivals for h > 0 (refer Table 3.1). If the source is not at the middle of the channel, M.E. increases with h. For range 1000, the M.E. initially decreases with

h, because there are no new arrivals and the only one τ_i is present and this increases with h (refer Table 3.1). For range 500m, the M.E. decreases inversely proportional to h, because there are only two rays in RB1 and as 'h' increases the second ray moves out of RB1.

Now we propose the following conclusions:

M.E. is a function of both target range and 'h'; in other words M.E. is a function of number arrivals in RB1 and the amount of net overlap in RB1. We also observed from equation (3.66) that P_D is directly proportional to M.E., for a given P_A and SNR. We now propose that if the source is in the middle of the channel, the M.E. is minimum and therefore the improvement on P_D is also proportionally less. If the source is not in the middle of the channel, the detection probability is markedly larger at long ranges as h increases and reverse the case for short ranges. For a given source power, SNR decreases with range and we can effect a reduction in source power to an order of 6 dB if the target is detected with source located at maximum possible h at long ranges. For short ranges irrespective of range, we have approximately 2 dB reduction due to M.E.

3.5.1 Comparison of Conventional receiver performance with performance bounds of optimum receivers in Sec. 3.3 and 3.3.3:

We computed the performance bounds of the receivers suggested in Section 3.3 and 3.3.3 i.e, for receivers where delay times are perfectly known. The receiver in Sec. 3.3 is having rectangular transmitting pulse, where as the one in Sec. 3.3.1 is having modulated transmitting pulse which will result in mutually orthogonal signal waveforms along different paths. The performance bounds are calculated following the development in Sec. 3.3.2. For the same false alarm the probability of miss for conventional receiver in Sec. 3.4 is also computed. The results are tabulated in Table 3.2. The parameter values used are arbitrary but similar results hold good for all sets of parameters of interest.

The following inferences are made:

1. The degradation in conventional receiver cannot be exactly found as the performance results corresponding to the optimum receiver are bounds. For a given P_F and SNR, the P_M of conventional receiver is always less than that of optimum receivers. Hence the conventional receiver in Sec. 3.4 offers satisfactory performance.
2. The conventional receiver designed for the receiver discussed in Sec. 3.3.3 will offer no improvement over the conventional receiver designed then the channel is thought to be unbounded.

Table 3-1 : Number of Signal waveforms arriving in 1st range bin

Range	NUMBER OF ARRIVALS in RB1.				
	h = 0m.	h = 50m	h = 100m	h = 150m	h = 200
500m	2	2	2	2	1
1000m	2 (3)*	2 (3)	3	3	4
1500m	2 (3)	3	4	4	4
2000m	3 (4)	4	4	4	4

* The number in brackets indicate the number of arrivals when the source is at the middle of the channel

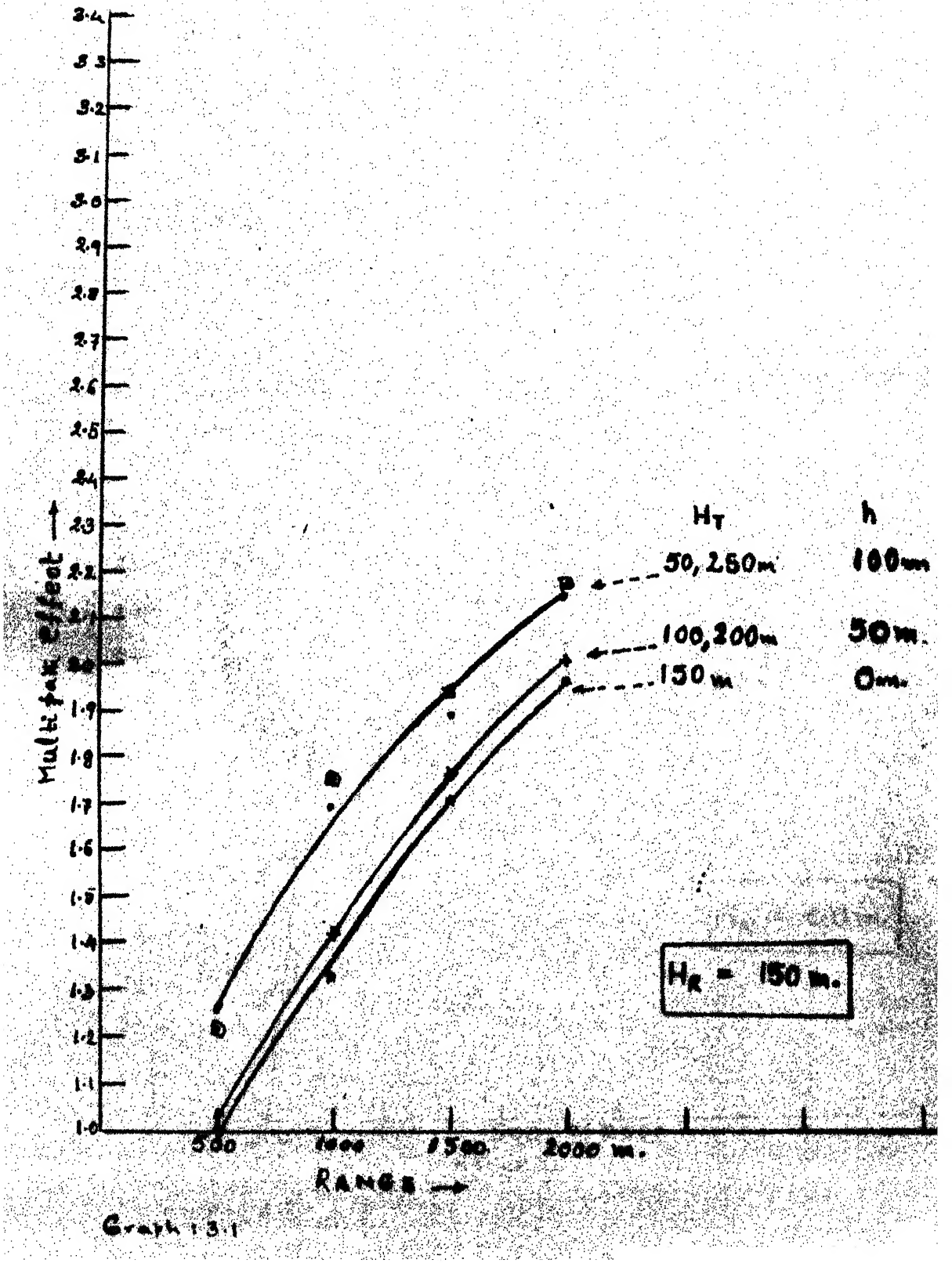
Multipath effect
2·4
2·3
2·2
2·1
2·0
1·9
1·8
1·7
1·6
1·5
1·4
1·3
1·2
1·1
1·0
500
1000
1500
2000 m.
RANGE →
H_T
h
50, 250m
100m
100, 200m
50m.
150 m
0m.
H_R = 150 m.

Graph : 3.1

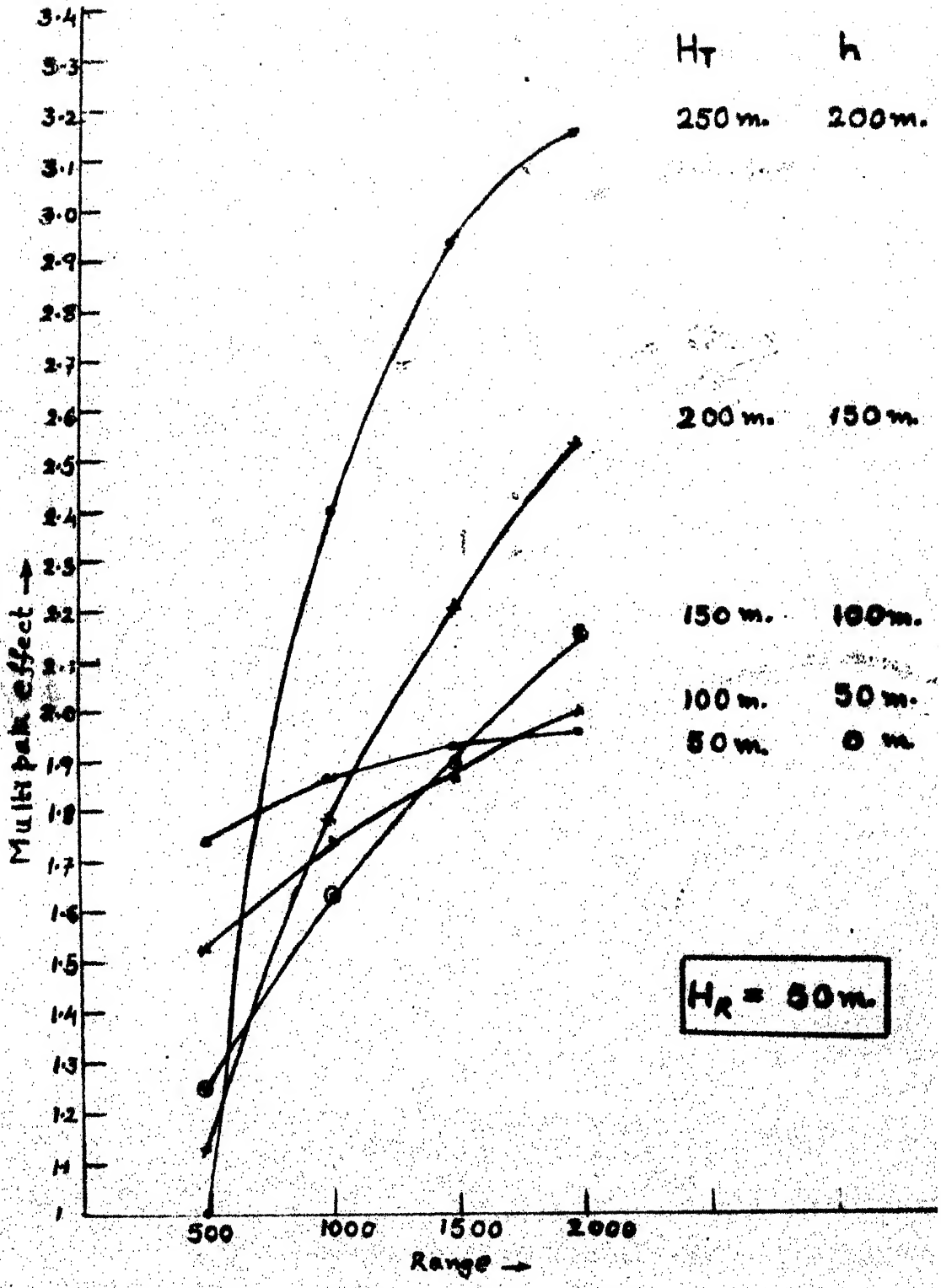
3·4
3·3
3·2
3·1
3·0
2·9
2·8
2·7
2·6
2·5
2·4
2·3
2·2
2·1
2·0
1·9
1·8
1·7
1·6
1·5
1·4
1·3
1·2
1·1
1
Multi path effect →
500
1000
1500
2000
Range →
H_T h
250 m. 200 m.
200 m. 150 m.
150 m. 100 m.
100 m. 50 m.
50 m. 0 m.
H_R = 50 m.

Graph 3·2.

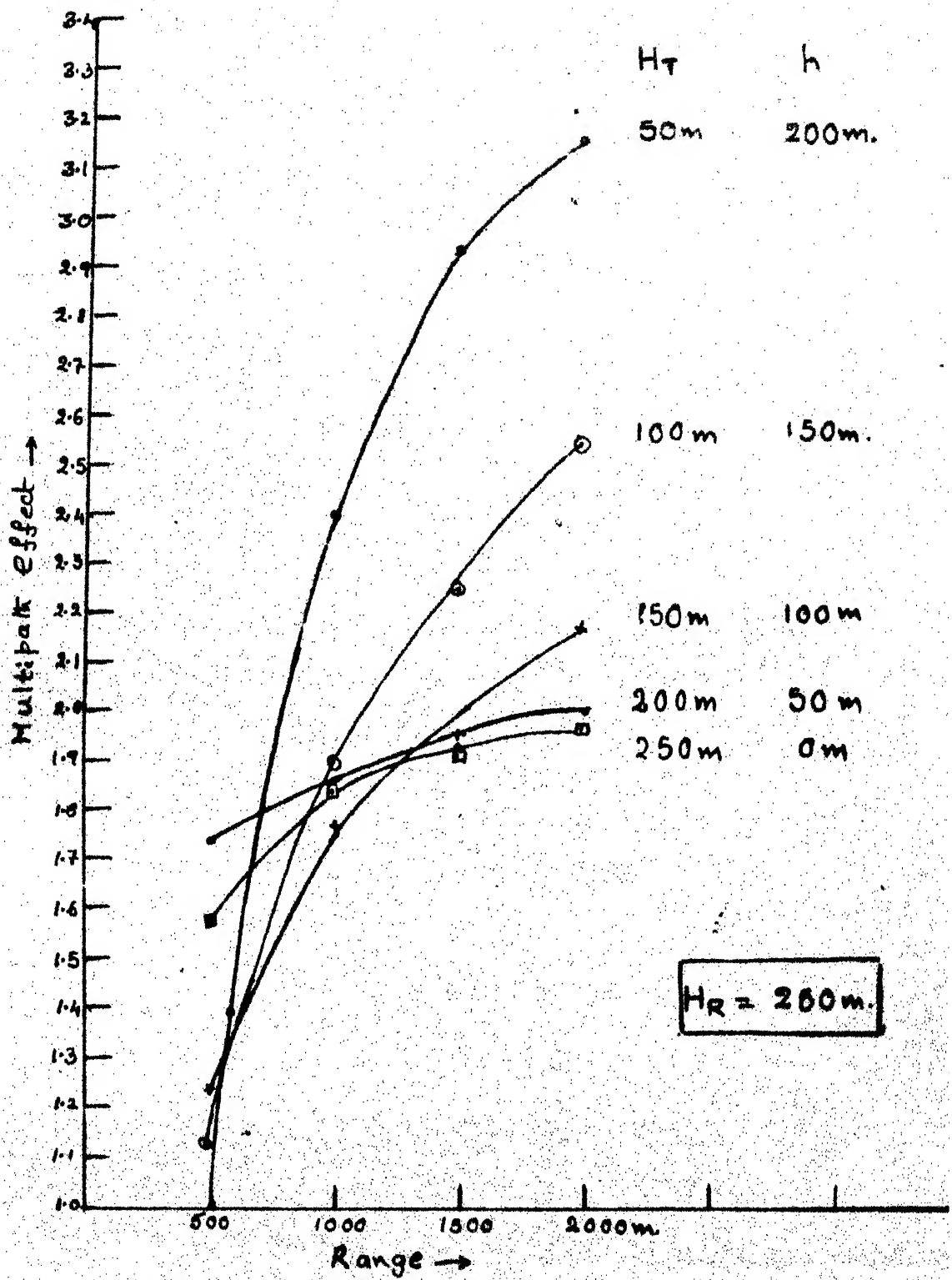
Multipath effect →
3·4
3·3
3·2
3·1
3·0
2·9
2·8
2·7
2·6
2·5
2·4
2·3
2·2
2·1
2·0
1·9
1·8
1·7
1·6
1·5
1·4
1·3
1·2
1·1
1·0
500
1000
1500
2000m.
Range →
H_T h
50m 200m.
100m 150m.
150m 100m
200m 50m
250m 0m
H_R = 200m.

Graph 3·3 :

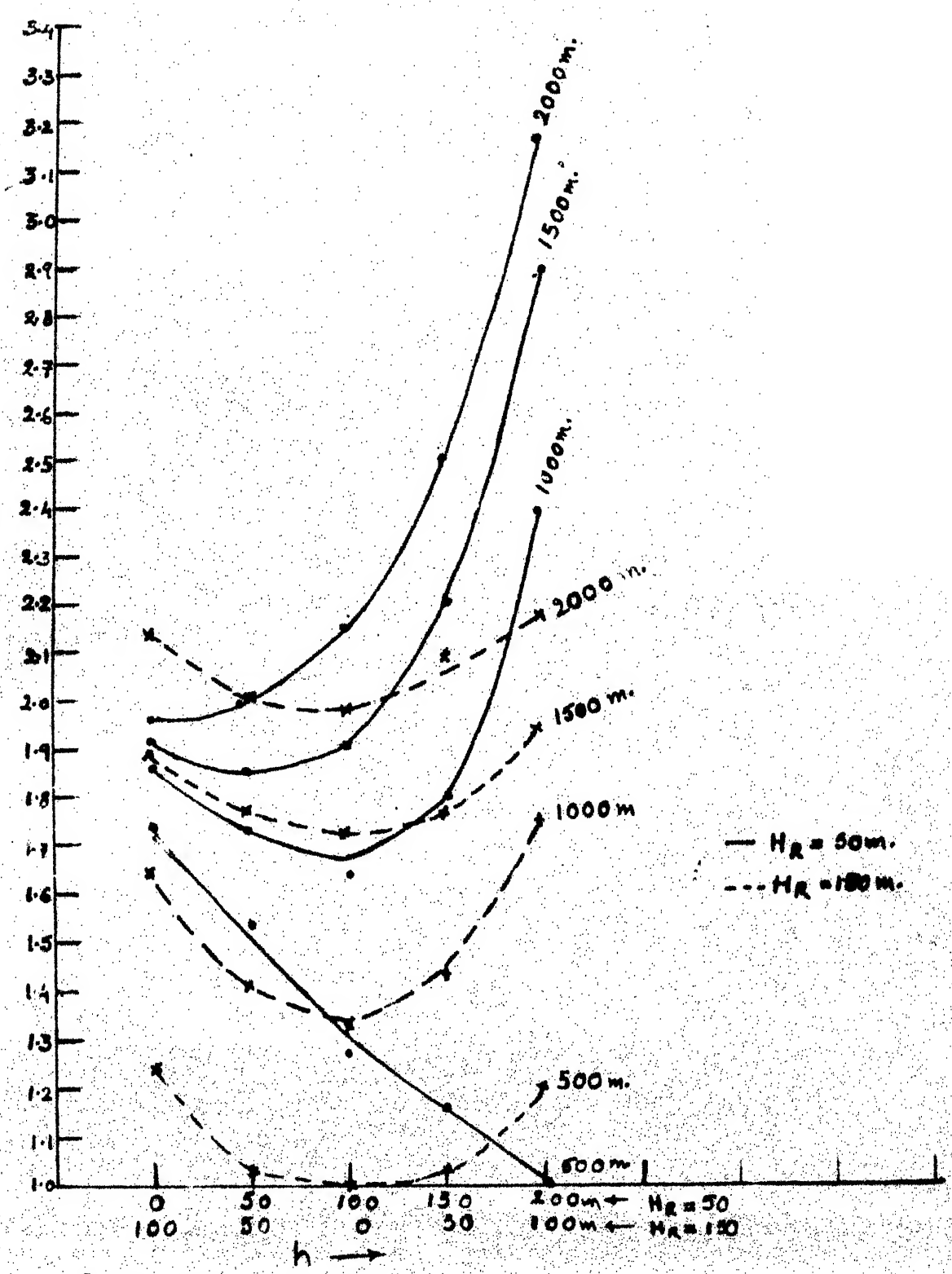
3·4
3·3
3·2
3·1
3·0
2·9
2·8
2·7
2·6
2·5
2·4
2·3
2·2
2·1
2·0
1·9
1·8
1·7
1·6
1·5
1·4
1·3
1·2
1·1
1·0
2000m.
1500m.
1000m.
2000 m.
1500 m.
1000 m
500 m.
500m
— H_R = 50m.
--- H_R = 150 m.
0 50 100 150 200m ← H_R = 50
100 50 0 50 100m ← H_R = 150
h →

Graph 3·4

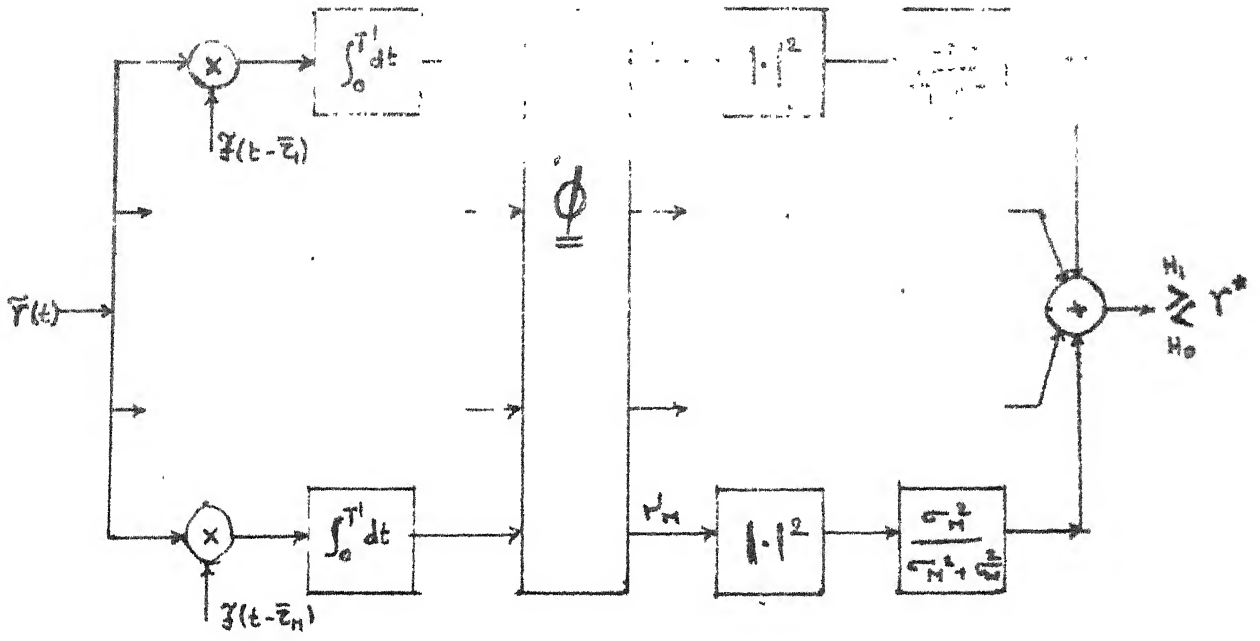

FIG 3·1: optimum receiver for rectangular transmitting pulse.

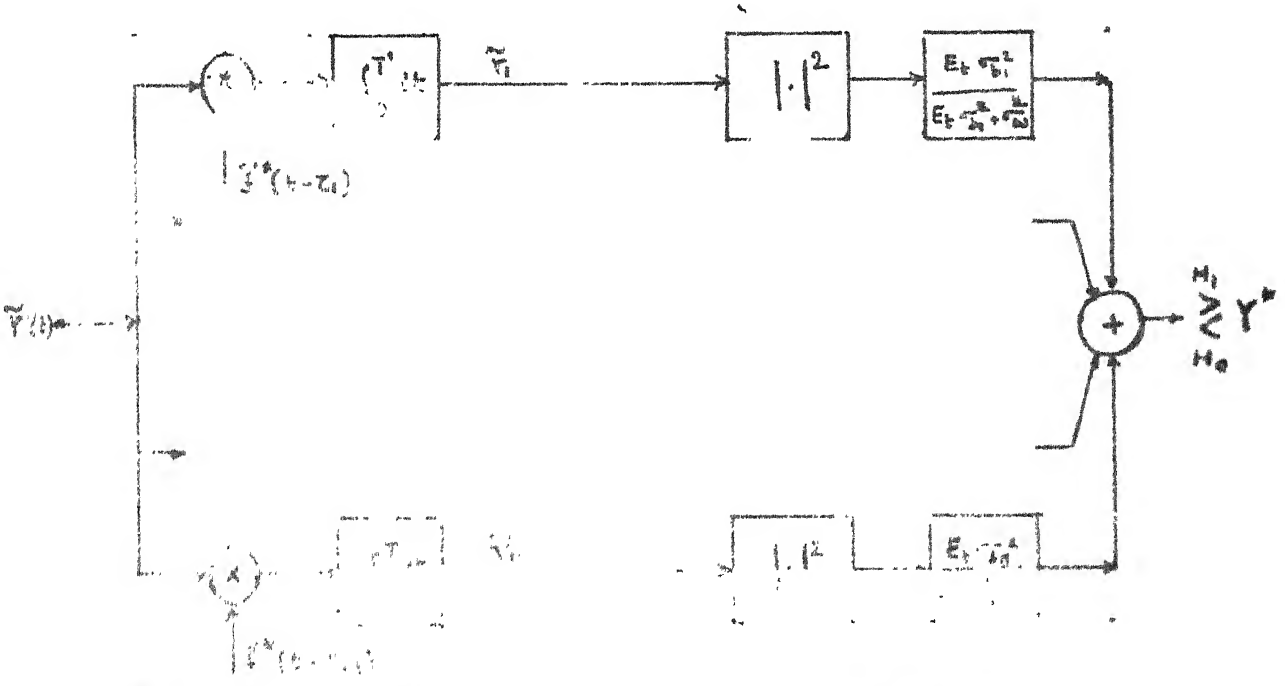

FIG 3·2: Optimum receiver for Coded transmitting pulse

CHAPTER 4

CONCLUSIONS

In this thesis we made an attempt to model the shallow water targets, and then we investigated some receiver structures for detecting them under white noise conditions by an active SODAR.

Towards this, we have used ray theory to develope the acoustic transmission in shallow waters and it resulted in a discrete multipath structure. Each ray path is characterized by parameters; travel time, spreading loss, and boundary loss and phase shift. Hence the received signal energy is the superposition of signal energies arriving along different paths after getting reflected from the target. We have seen the number of ray paths that contribute significant energy at the receiver are limited by SODAR beam pattern and critical angle associated with bottom reflection. We then analysed the variations in total loss suffered by a ray and it's travel time with respective different ranges of target from receiver, for source depth and target depth.

For an iso-speed channel, assuming target velocity to be much smaller than sound velocity and channel depth

to be much smaller than direct ray range, we obtained the linearized model for the received signal for a SODAR from a moving target. The received signal energy was interpreted to be same as that of a stationary target with doppler shift in carrier frequency independent of number of rays that contribute at receiver. This common doppler shift for the composite signal allows us to look for a simple receiver configurations.

The detection problem for the shallow water target by SODAR is formulated. We assumed the combined effect of path losses, boundary losses and losses due to reflection at target as attenuation coefficient of the signal arriving along the path and it is modelled as zero mean complex Gaussian random variable. If the arrival times are also treated as random variables, then the optimum receiver for this characterization is practical only at high signal to noise ratios. Assuming perfect knowledge of the time of arrivals, the optimum receiver was investigated and analysed. The conventional receiver for this characterization found to,be adequate. Usage of special signal waveforms (Barker coded, LFM etc.) for transmitter pulse resulted in simpler optimum receiver structure. But the conventional receiver for this specifications gives no additional advantages.

Suggestions for Future Work:

As an extension of the work done in this thesis an appropriate model for the channel where the sound velocity is a function of depth and the boundaries are of complex structure. The target may also move along any specified path.

The model may also include the effects of reverbaration which then will be more realistic. An appropriate model for the arrival to times may be attempted to obtain an optimum receiver in a composite hypotheses situation.

For the optimum receiver analysed in Section 3.2, we assumed to have perfect knowledge of time delay differences. Some efficient estimation methods may be investigated. One possible way of estimating travel times is as so follows:

With an apriori knowledge of approximate range and receiver depth, the time delay differences (τ_i) may be modelled as uniformly distributed random variables. If $\Delta_i = \tau_{i\,max} - \tau_{i\,min}$. If T_o is the correlation time of the transmitting signal and $KT_o = \Delta_i$, then using a scheme shown in Fig. 4.1 we may estimate time delays.

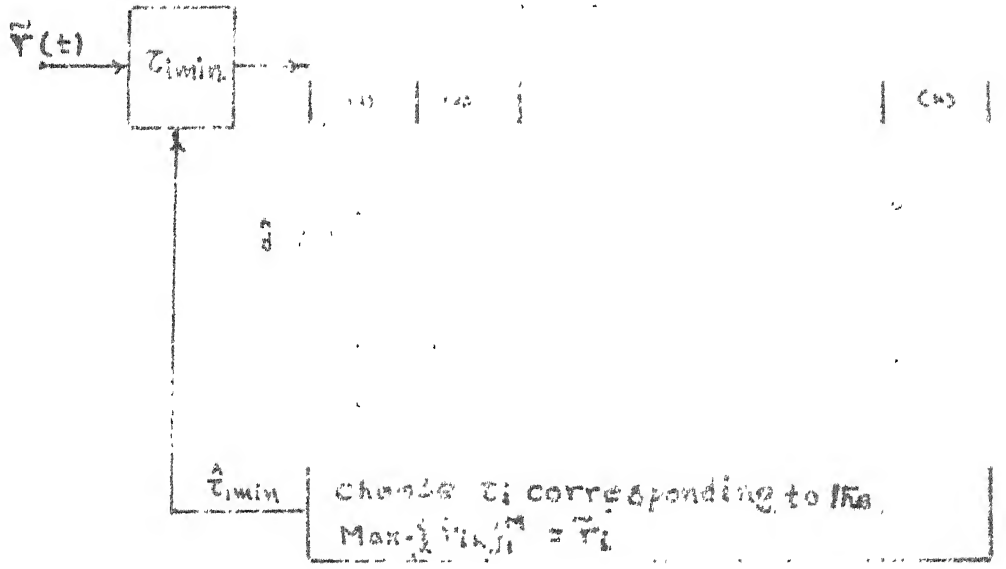

Fig: 4.1 Estimation of time delay diffe

REFERENCES

1. R.P. Flanuagan, N.L. Weinberg and J.C. Clark: 'Coherent analysis of ray propagation with moving source and fixed receiver', J. Acoustic Soc. Am. 56, 1673-1680 (1974).

2. A.A. Gerlach: 'Motion introduced coherence degradation in passive systems', IEEE Trans. on ASSP, vol. 26, pp. 1-9, Feb. 1978.

3. A.A. Gerlach: 'Impact of the ocean acoustic transfer function on the coherence of under sea propagation', IEEE Trans. on ASSP, vol. 28, pp. 145-157, Apr. 1980.

4. J.C. Hassab: 'Passive tracking of a moving source by a single observer in shallow water', Journal of Sound and Vibrations, 44(1), pp. 127-145 (1976).

5. G.M. Jacyna, M.J. Jacobson and J.G. Clark: 'General treatment of source motion on the total acoustic field with application to an iso-speed channel, J. Acoust. Soc. Am., vol. 60, pp. 815-824, Oct. 1976.

6. Lev. A. Chernov: Wave propagation in random medium, McGraw-Hill, 1960.

7. A.D. Pierce: Acoustics : An introduction to it's physical principals and applications, McGraw-Hill,1981.

8. C.B. Officer: Introduction to the theory of 'Sound Transmission' with application to the ocean, pp. 117-145, McGraw-Hill, 1958.

9. C.B. Officer: Introduction to the theory of 'Sound Transmission' with application to the ocean, pp. 89-116, McGraw-Hill.

10. C.B. Officer: Introduction to the theory of 'Sound Transmission' with application to the ocean, pp. 51, McGraw-Hill.

11. Robert J. Urick, Principles of under water sound, McGraw-Hill,1967.

12. C.T. Tindle and G.E.J. Bold; Improved ray calculations in shallow water, J. Acoust. Soc. Am. pp. 813-819, Sept. 1981.

13. L.M. Brekhovskikh; Waves in layered media, Academic Press (1980).

14. M.J. Jacobson; Analysis of spreading loss for refracted/reflected rays in constant velocity gradient media, J. Acoust. Soc. Am. pp. 2298-2305, Dec. 1964.

15. G.V. Anand and P. Balasubramanian: Sound transmission in coastel seas: Report O-22, Dept. of Elec. Comm. Engg., Indian Institute of Science (Nov. 1983).

16. H.L. Van Trees, 'Detection, estimation and modulation theory, vol. 1, Chapter 2.

17. H.L. Van Trees, Detection, estimation and modulation theory, vol. 1, Chapter 2.7.